PAUL SCHERRER INSTITUT

PSI

Annual Report 2019

Electrochemistry Laboratory

Cover
Micro-CT of Binder in SGL Gas
Diffusion Layer (GDL).

PAUL SCHERRER INSTITUT

PSI

Annual Report 2019

Electrochemistry Laboratory

A full version of this report is also available on the web
http://www.psi.ch/lec

CONTENTS

EDITORIAL

PSI's Electrochemistry Laboratory is the leading center for research in electrochemical energy storage and conversion in Switzerland. The Lab bridges fundamental electrochemical science with applied electrochemical engineering, which is unique even on international standards. This allows us to keep a systemic view even when addressing basic scientific questions.

In this Annual Report 2019, you will not only find details on PSI's Electrochemistry Laboratory, but six reports on actual topics of the Lab, contributing to the grand challenges of electrochemical energy storage and conversion. Further the Laboratories key facts and figures for 2019 are given, including a full list of our 46 peer reviewed publications and numerous talks demonstrating the leading role of PSI's Electrochemistry Laboratory on the national and international level.

In April 2019, the Lab held the 35th annual Swiss Electrochemistry Symposium *On the role of batteries in future energy systems* with world-class scientists and engineers as speakers, attracting an audience of more than 120 participants. Details of this event you will find also in this annual report on page 40.

2019 was also a successful year for eleven of our PhD students who successfully defended their theses. The new PhDs mostly continued their careers directly either in an academic or industrial environment.

At this point it needs to be mentioned that all our projects and results could not have been achieved without the funding we received over the years from industrial partners and the different funding agencies in Switzerland and abroad. We, therefore, would like to take this opportunity to thank all our funding sources hoping to continue our successful collaborations in the years to come.

In 2019, however, also important changes occured. The structure of the Lab was reorganized, in order that we are now organized in six groups. The change secures a smooth transition into a successful future.

Felix N. Büchi

THE ELECTROCHEMISTRY LABORATORY AT A GLANCE

Our Mission

Advancing electrochemical energy storage and conversion by

- **developing novel electrochemical materials, cells and devices;**

- **using novel, advanced *in situ* and *operando* methods;**

- **performing fundamental, applied and industry-oriented research.**

PSI's Electrochemistry Laboratory is Switzerland's largest Center for Electrochemical Research with about 70 employees. Our mission is to advance the scientific and technological understanding of electrochemical energy storage and conversion specifically in the context of a sustainable energy system, where renewable energy is required to be stored in secondary batteries or chemicals such as hydrogen and (re-)converted into electricity. The Laboratory's R&D, is hence focused on secondary batteries – specifically Li- and Na-based systems –, polymer electrolyte fuel cells and electrolyzers, as well as redox flow cells.

As a research institute's laboratory we are bridging the gap between fundamental science and applied engineering by combining both academically and industrially relevant questions. For the technologies under research, we not only develop fundamental understanding of materials on an atomic and molecular scale (electrochemical materials sciences and electrocatalysis), but also in the applied development of technical cells and devices, e.g., fuel cell systems.

On many technical complexity levels, we are developing and utilizing advanced *in situ* and *operando* diagnostic tools to gain insights in properties and processes from the nanometer to the centimeter scale, respectively, making intensive use of PSI's unique large scale facilities such as the Swiss Light Source (SLS) and the Swiss Neutron Spallation Source (SINQ).
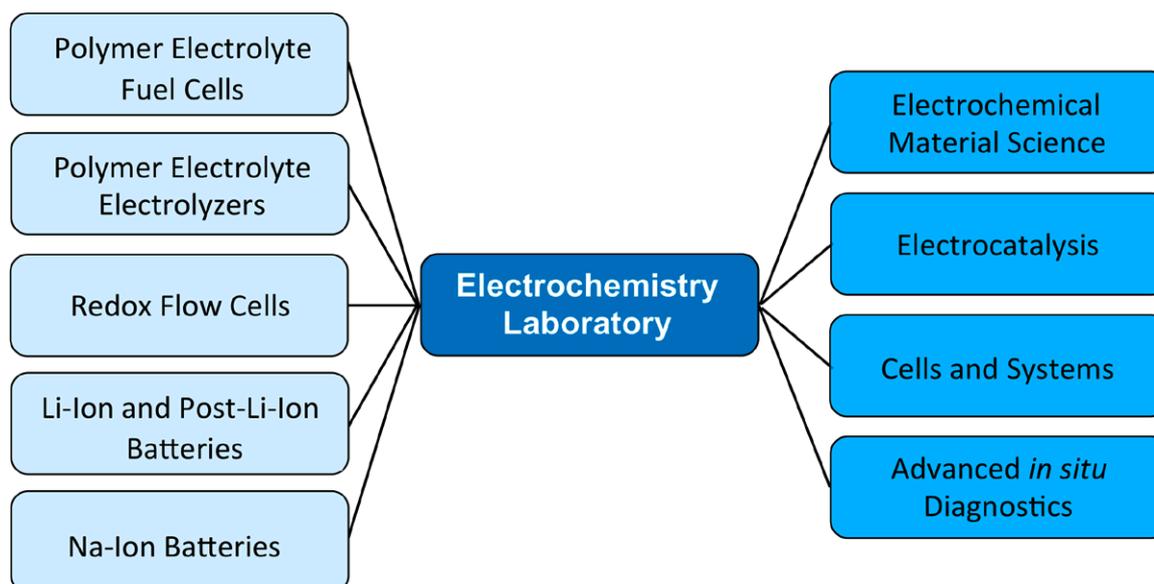
Electrochemical energy storage

The vision in Electrochemical Energy Storage is to make significant contributions to the most advanced electrochemical energy storage systems.

The work is focused on rechargeable batteries, which are mainly lithium and sodium based. The scientific goal is a profound understanding of the electrochemical processes in complex non-aqueous systems. In particular, of utmost scientific interest are the numerous interactions of all components determining the safety and life time of such systems.

Introducing IAESTE intern to assembly of Na-cells.

The work equally considers the synthesis of novel materials for electrochemical energy storage and the modification of known materials (e.g., carbon), and material characterization, keeping in mind the entire span from basic science to industrial applications. To answer the scientific questions, we develop various sophisticated *in situ* and *operando* methods for use in the field of non-aqueous solid-state electrochemistry and investigate the physical and electrochemical properties of insertion and conversion materials and electrochemical interfaces *in situ*. Also, we do electrochemical engineering work on three-dimensional electrodes and characterize industrial batteries.

Electrochemical energy conversion

The Electrochemical Energy Conversion focuses on the development and in-depth understanding of materials, processes and devices for the conversion of renewable power to hydrogen (or syngas) and back to power. Especially in the context of a sustainable energy system utilizing hydrogen as an energy carrier, these electrochemical energy conversion steps are of particular importance.

In this topical context the work is focused on Polymer Electrolyte Fuel Cells (PEFC) and Polymer Electrolyte Water Electrolyzers (PEWE) for water electrolysis and the co-electrolysis of CO_2 and water, respectively. In addition, work is devoted on the materials development for Redox Flow Cell systems.

The R&D strategy involves activities on four pathways:
- the development and application of advanced *in situ* and *operando* diagnostic imaging tools on stack, cell and component levels (X-rays and neutrons);
- membrane development based on PSI's own radiation-grafting technology;
- research in electrocatalysis and the reaction kinetics of the relevant reactions (e.g., the oxygen electrode reactions) for improved understanding of intrinsically limiting factors; and
- system, stack and cell engineering.

On the level of technology demonstration, we have designed and we develop and operate the so-called hydrogen path on PSI's Energy System Integration (ESI) Platform on the 100 kW level, i.e., operate a technical scale PEWE System including product gas clean-up and a H_2-O_2 PEFC reconversion system, which is based on a joint development with our collaboration partner Swiss Hydrogen SA.

In 2019, the PSI Spin-off Gaia Membranes was founded, with the aim of commercializing PSI's radiation grafted membrane technology. The target applications are vanadium redox flow batteries and water electrolyzers.

Setting up a new grafting reactor for the scaled-up production of Amphion™ membranes for vanadium redox flow batteries.

CURRENT SCIENTIFIC TOPICS

Recent developments in imaging techniques for Li-ion battery applications: The case of XPEEM and neutron imaging

The continuous need for increasing the electrochemical performance and safety of Li-ion batteries (LiBs) requires an incessant development of characterization techniques capable of providing better insights into the physics and chemistry of the various parts of the battery. Both the bulk and the surface modifications of the electrodes need to be investigated upon cycling, since they both have a direct impact on the battery performance. In this context, XPEEM and neutron imaging have been adapted to investigate the surface and the bulk evolution of cycled electrodes.

Understanding the different reactions taking place inside a Li-ion battery (LIB) device, in particular in the bulk or at the interface between the carbonate-based electrolytes and the various particles of the electrode, remains crucial for the development of stable, efficient, and safe batteries. In the following report we present the importance of imaging techniques such as the X-ray photoemission electron microscopy (XPEEM) and neutron imaging to elucidate fundamental reactions related to the electrolyte decomposition, structural degradation, and Li-ion transport limitations upon cycling.

XPEEM nanoscale spectroscopy on LIB electrodes

XPEEM is a synchrotron-based surface characterization technique which relies on the availability of a tunable and brilliant X-ray source. It is widely used to study the chemical, electronic, and magnetic properties of a broad range of materials. In XPEEM, the sample is uniformly illuminated with a monochromatic X-ray beam where the local intensity of secondary emitted photoelectrons (proportional to the X-ray absorption of the material) is imaged using electron optics. By varying the energy of the incoming photons, local elemental maps of the sample can be obtained with a spatial resolution better than 70 nm. The limited escape depth of the secondary electrons from materials, in the range of 2–3 nm for low energy electrons, makes this technique very surface sensitive and particularly well suited for the study of surfaces and interfaces. Another intrinsic advantage of XPEEM resides in its non-destructive nature. For battery application a commercial-like electrode can be transferred to the microscope without prior sample thinning or grinding or changing the working environment of the particles.

One case study is presented in this report performed on a $Li_4Ti_5O_{12}$ (LTO) electrode, to highlight the advantage of combining lateral resolution and surface sensitivity with chemical information. From the point of view of surface reactivity, LTO, a material designed for high power cells, shows a high (de-)lithiation potential plateau at 1.55 V vs. Li^+/Li that lies within the expected thermodynamic stability window of the carbonate-based electrolytes. Although electrolyte reduction is not expected to occur at this potential, the release of gas associated with electrolyte decomposition is known to occur, in particular when LTO is cycled above 50° C. [1] The excellent lateral resolution and surface sensitivity of XPEEM are exploited to solve this enigma, especially when coupled with supporting techniques, such as density functional theory (DFT) calculations. [2] Since the electrolyte decomposition by-products contain carbonate species, we can detect their presence by acquiring elemental maps at the carbonate peak located at 290.4 eV (Figure 1).
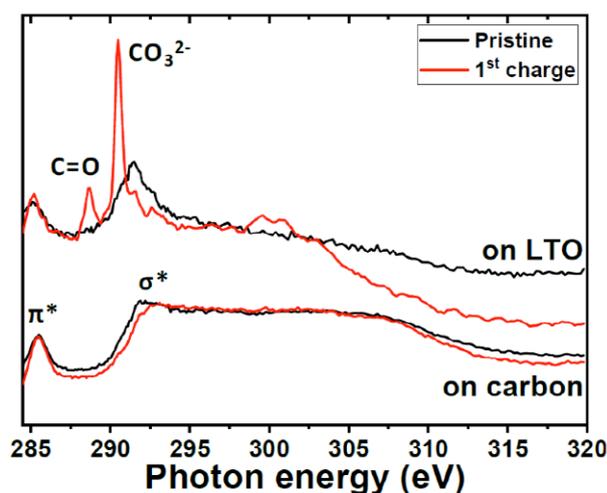
Figure 1. C K-edge XAS spectra acquired from the LTO electrode at the pristine (black) and lithiated (red) state on carbon and LTO particles, respectively.

Figure 2 shows the elemental map of a lithiated LTO electrode, where LTO particles are highlighted in blue (contrast image at the Ti L-edge/pre-edge), conductive carbon in red (contrast image at the C K-edge/pre-edge), and the carbonates in yellow. It is clearly observed that the electrolyte decomposition by-products only grow on the LTO particles, while the carbon areas show no carbonate signal. Local XAS spectra (Figure 1) confirm the presence of carbonates solely on the LTO particles despite the comparatively high working potential of 1.55 V vs. Li^+/Li, as reported in detail by Leanza et al. [2]. With the support of DFT calculations, we demonstrated that this behaviour is caused by the solvents adsorbed on the LTO outer planes driven by the Li-ion insertion. The DFT results indicate that Li-ion insertion leads to a shift of the LUMO of the adsorbed solvents to energies below the Fermi level position of lithiated LTO and thus to chemical instability.

The microscopy and local spectroscopy capabilities of XPEEM have been also the key for elucidating the complex reactions at the surface of various cathode materials such as Li-rich NCM together with their impact on the counter electrode. Those results are reported in the papers of Daniela Leanza et al. [3, 4].

In this report we want to emphasize that XPEEM is a unique technique which can assess the preferential reactions of the electrolyte on the active material particles unquestionably by combining the high lateral resolution and surface sensitivity with spectroscopy data.
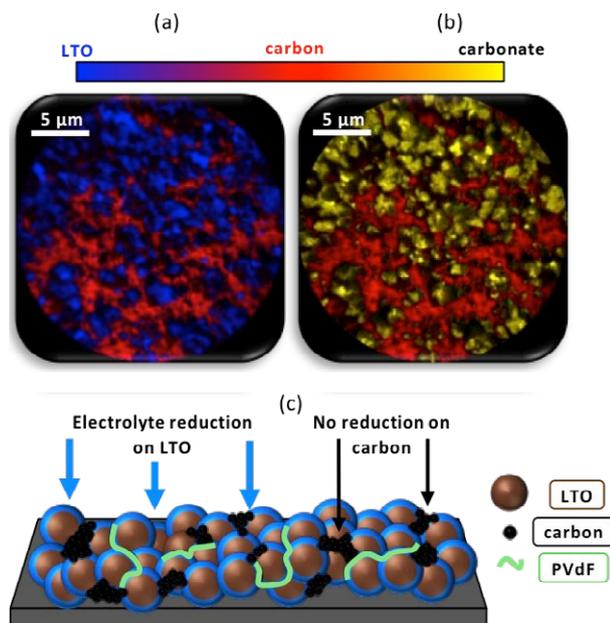
Figure 2. (a) Elemental map of a lithiated LTO electrode, showing the complementary position of LTO (blue) and carbon (red) particles. (b) Carbonates (yellow) do not cover the carbon particles (red), confirming that carbonates are only formed on the LTO surface. The proposed mechanism leading to the electrolyte decomposing only on the LTO particles is shown in (c).

Neutron imaging of LIB electrodes

Unlike methods which indirectly investigate the impact of lithium insertion (e.g. as a change in diffraction pattern or in material density), the use of neutrons allows a direct probe of the concentration of lithium atoms. This is due to the very high absorption cross section of the ^{6}Li isotope, which represents a non-negligible fraction of approximately 7.5 % of the natural lithium composition. Imaging with neutrons has the potential to resolve the state of charge distribution not only over the area of the cell, but also across the electrode thickness. This is of particular importance to elucidate limitations related to the transport of Li ions across the electrode, which can have a particular importance for fast charging and discharging.

However, imaging across electrodes requires a sufficiently high resolution. To this purpose, we can count on the fact that PSI is a leading institution in the field of high-resolution neutron imaging since 15 years. The developments realized within the Neutron Imaging and Applied Materials Group (NIAG, LNS laboratory) included the integration of specialized optics and novel scintillator screens based on enriched gadolinium, resulting in reaching a resolution below 10 μm while keeping a very good detection efficiency [5].

Furthermore, as a collaboration between the Electrochemistry Laboratory and the NIAG group, the application to imaging of electrochemical systems (and in particular of fuel cells) has been a strong driver to develop anisotropic setup specifically tuned for imaging with resolution requirements highly differing in the directions along and across the cell structure [6].

An example (see Figure 3) illustrates the application of this approach. A Li-ion battery using a conventional liquid electrolyte was used with a rectangular shaped electrode. The combination of a very high resolution across the electrode with a field of view large enough to image the electrode length (20 mm)

in the perpendicular direction was obtained by using our anisotropic resolution enhancement method based on a tilted detector and anisotropic beam collimation [6].

Because enhancing resolution in only one direction is less costly in terms of temporal resolution loss, and using isotope contrast enhancement, we could obtain images of the Li distribution within less than 3 minutes, making the method suitable for fast charge/discharge imaging.
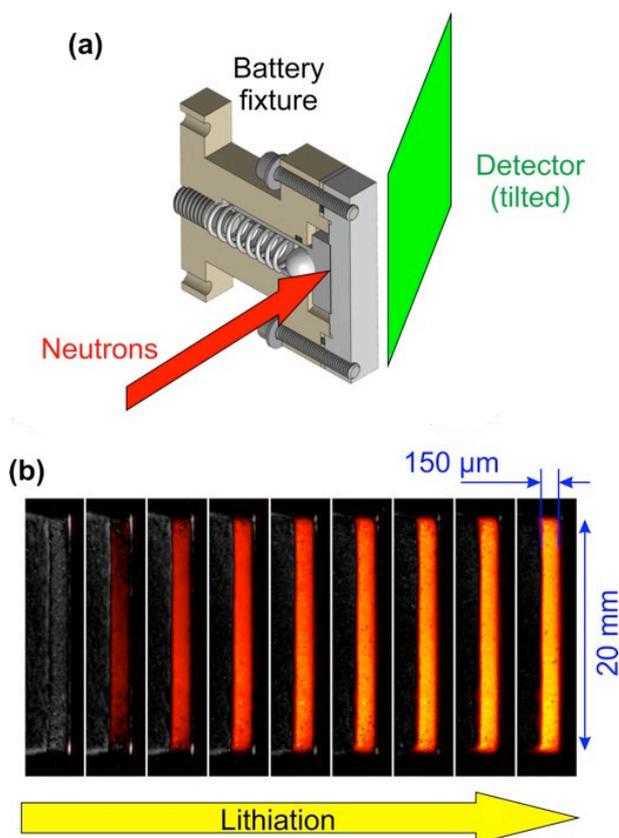
Figure 3. (a) Illustration of the anisotropic setup used for imaging. (b) Imaging of the lithium distribution during lithiation (150 μm thick electrode). The integral exposure for each of the images is 2.5 min.

When using conventional white beam imaging, the contribution from the Li atoms and from H atoms included in the electrolyte are superposed. The use of isotope enrichment allows to minimize the influence of the electrolyte, but a further possibility is offered by the different neutron wavelength dependence of the hydrogen and lithium cross sections. Wavelength resolved imaging can be obtained using the time-of-flight method either at pulsed neutrons sources, or by chopping the neutron beam.

Recent work realized on time-of-flight imaging for the distinction of water and ice in fuel cells [7] demonstrated that this technique can be applied with a limited loss in neutron flux, as long as only a coarse wavelength resolution is required. In the frame of an ongoing project, we are applying this approach to deconvolute the contributions of the lithium movement and electrolyte redistribution. First measurements (Figure 4) on reference samples (lithium metal and carbonate electrolyte) allowed to confirm the wavelength dependency of the cross sections, opening the way to future *in situ* measurement with this method.

(a)

(b)
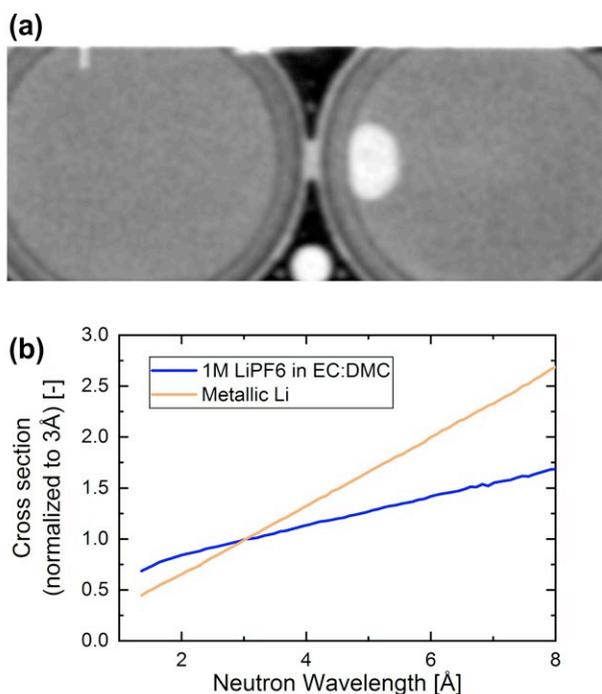
Figure 4. *(a) Neutron images of test coin cells used for electrolyte cross section measurements. (b) Measured cross sections for a standard battery electrolyte (1m LiPF$_6$ in EC:DMC) and for lithium. The cross sections are normalized to their value at 3 Å for a better comparison of the wavelength dependency.*

Conclusions

Investigating the surface and the bulk of Li-ion battery electrodes is a challenging task, mainly due to the complexity of the chemistry inside the battery and the limited number of non-destructive techniques. Here we have demonstrated how XPEEM can be used to investigate the surface evolution at the level of individual particles of the electrode in their working environment, by coupling morphological and chemical information from the electrode's surface. We anticipate that a similar approach can be applied to other processes of insertion materials, such for high-voltage cathodes, where the knowledge of their interfaces and the mechanisms involved in surface layer formation and other redox processes is still rather poor. In addition, the optimization of XPEEM for the study of battery electrodes provides a strong motivation to push this technique for *operando* measurements and to contribute to a better engineering of battery electrodes. Neutron imaging was shown to be a highly versatile tool for probing the lithium distribution across electrodes. Because neutrons directly probe the distribution of Li atoms – unlike other methods based on the change of crystalline structure for example – their application is not limited to a particular electrode type, but allows tracking the lithium fate in any type of batteries.

Contact

For further information on the techniques, please contact Dr. Mario El Kazzi, Head of the Group *Battery Materials and Diagnostics,* and Dr. Pierre Boillat, Head of the Group *Neutron Radiography of Electrochemical Systems.*

mario.el-kazzi@psi.ch
pierre.boillat@psi.ch

Contributors

The contributors for this particular research topic are
on XPEEM: Daniela Leanza, Marta Mirolo, Carlos A.F. Vaz, Petr Novák;
on neutron imaging: Ricardo Carreon, Magali Cochet, Laura Höltschi, David McNulty, Manuel Morgano, Sebastien Sallard, Muriel Siegwart, Markus Strobl, Sigita Trabesinger, Pavel Trtik, Claire Villevieille, Eric Winter.

Acknowledgement

References

[1] M. He, E. Castel, A. Laumann, G. Nuspl, P. Novák, E.J. Berg, *J. Electrochem. Soc.* **162** (6), A870–A876 (2015).

[2] D. Leanza; C.A.F. Vaz, I. Czekaj, P. Novák, M. El Kazzi, *J. Mater. Chem. A* **6** (8), 3534–3542 (2018).

[3] D. Leanza, M. Mirolo, C.A.F. Vaz, P. Novák, M. El Kazzi, *Batteries & Supercaps* **2** (5), 482–492 (2019).

[4] D. Leanza, C.A.F. Vaz, G. Melinte, X. Mu, P. Novák, M. El Kazzi, *ACS Appl. Mater. Interfaces* **11** (6), 6054–6065 (2019).

[5] P. Trtik, E.H. Lehmann, *Journal of Physics: Conference Series* **746**, 012004 (2016).

[6] P. Boillat, G. Frei, E.H. Lehmann, G.G. Scherer, A. Wokaun, *Electrochem. Solid-State Lett.* **13** (3), B25–B27 (2010).

[7] M. Siegwart, R. Woracek, J.I. Márquez Damián, A.S. Tremsin, V. Manzi-Orezzoli, M. Strobl, T.J. Schmidt, P. Boillat, *Review of Scientific Instruments* **90**, 103705 (2019).

Development towards next generation water electrolyzers

Decarbonization of the energy system across different sectors (Power-to-X) relies heavily on the availability of low-cost hydrogen produced from renewable power by water electrolysis. The reduction of the production cost of hydrogen is essential for the technology to be economically viable in providing fuel for mobility applications or feedstock for the chemical industry. The cost of hydrogen produced by the electrochemical splitting of water is dominated by the up-front cost of the electrolyzer and the conversion efficiency. This contribution summarizes our research on materials and components for next-generation water electrolyzers and highlights a novel method for the recovery of a metal cation contaminated catalyst-coated membrane.

The global share of renewable electricity has been increasing steadily over the past decade. Whereas the decarbonization of the electricity sector is forseeable, other sectors with a large carbon footprint, such as the mobility sector and the chemical industry, are less straightforward to decarbonize. In many applications, carbon based energy carriers either offer key advantages over non-carbon based energy (e.g., aviation fuel), are inherent to the process (e.g., coke in the blast furnace), very convenient and cheap, or a combination thereof.

Deep decarbonization of our economy, on the one hand, calls for substitution of energy carriers; for instance through replacement of internal combustion engine cars by battery or hydrogen fuel cell electric vehicles. The very traditional blast furnace process to produce iron and then steel could be replaced by iron produced by direct reduction (sponge iron process) using hydrogen. On the other hand, carbon is an important building block in the chemical industry. Here, carbon based feedstock and intermediates (e.g. syngas) can be produced from H_2 produced by water electrolysis from renewable electricity and CO_2 from renewable sources (e.g. biogas) or direct air capture.

Water electrolysis therefore forms a core technology in Power-to-Gas and Power-to-X scenarios. Future potential of these concepts depends largely on the economics of the process, which is determined to a large extent by the cost of hydrogen produced by water electrolysis. Among the different types of water electrolyzers, the polymer electrolyte water electrolyzer (PEWE) offers the prospect of high current density, differential pressure and dynamic operation. Figure 1 shows the key components and operating principle of a PEWE cell.

Current research and development is aimed at reducing the investment and operating cost. Investment cost can be reduced by using lower-cost materials and / or increasing the operating current density of the cell. The operating cost is mainly determined by the cost of electricity and the conversion efficiency, which is related to the operating cell voltage U_{cell}. The main loss terms in the electrochemical water splitting process in an acidic medium are the overpotential of the oxygen evolution reaction η_{OER} at the anode and the ohmic drop $i{\cdot}R$ across the membrane:

$$U_{cell} = U_0 + \eta_{OER} + i{\cdot}R + \eta_{mtx}$$

Mass transport limitations η_{mtx} to be also considered are related to the smoothness of the interface between catalyst layer and porous transport layer (PTL). Losses related to the cathodic reaction can be largely neglected due to the facile hydrogen evolution reaction (HER).
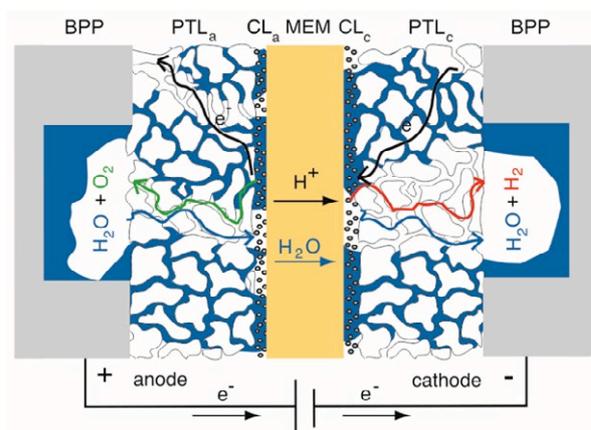
Figure 1. Schematic cross-section of an electrolysis cell, consisting of a membrane (MEM) coated with cathodic and anodic catalyst layer (CL_a, CL_c) sandwiched between two porous transport layers (PT_{La}, PT_{Lc}) and bipolar plates (BPPs).

Our research focuses on materials for next generation PEWE cells. In the following, work on advanced OER catalyst, membranes, and titanium PTL materials are highlighted. Moreover, we propose a novel regeneration method for contaminated PEWE cells using carbonic acid generated in the cathodic loop by injection of CO_2. This research contributes towards increasing the efficiency of the electrochemical water splitting process and thus reducing the projected cost of the produced hydrogen.

IrO_2/Nb_2O_5 based oxygen evolution electrocatalyst

It is well known that the oxygen evolution reaction (OER), taking place at the anode in a polymer electrolyte membrane water electrolyser (PEWE), is energetically demanding mainly due to its sluggish kinetics [1]. Given the extremely harsh conditions of operation (e.g. high potential and low pH), only few materials exhibit acceptable OER activity and stability. IrO_2 is one of the catalysts presenting the best compromise between activity and stability for OER and is therefore extensively studied [2]. Due to the scarcity of iridium, the current research focuses on reducing its quantity in the electrode while maximizing the catalytic activity. In this context, our strategy is to support low crystallite size IrO_2 particles on high surface area Nb_2O_5.

With this aim, we have investigated IrO_2 supported on Nb_2O_5 catalyst (Umicore®) and compared it to an unsupported IrO_2 catalyst with equivalent structure and morphology. As shown on HRTEM images (Figure 2a and b), both catalysts are com-

posed of agglomerated nanocrystals yielding a BET surface area of 10 m^2g^{-1}.

The electrochemical measurements, recorded in a standard rotating disk electrode setup, show that introducing Nb_2O_5 as a catalyst support maintains OER mass activity (9 A/g_{IrO_2} at 1.525 V vs. RHE) with slightly increasing stability (Figure 2c). Interestingly, the catalyst that contains Nb_2O_5 exhibits an increase in surface charge during the stability protocol, which is not observed for the unsupported catalyst (Figure 2d). Moreover, the general trend of surface charge decrease is shown for IrO_2 catalysts [3], meaning that this behavior is related to the interaction with the support.

These results have shown that using Nb_2O_5 as a catalyst support could be a potential way to reduce the Ir content on the anode side of a PEWE and, consequently, the catalyst cost. Further investigations are directed towards the understanding of the support influence and even greater reduction of the catalysts Ir content.
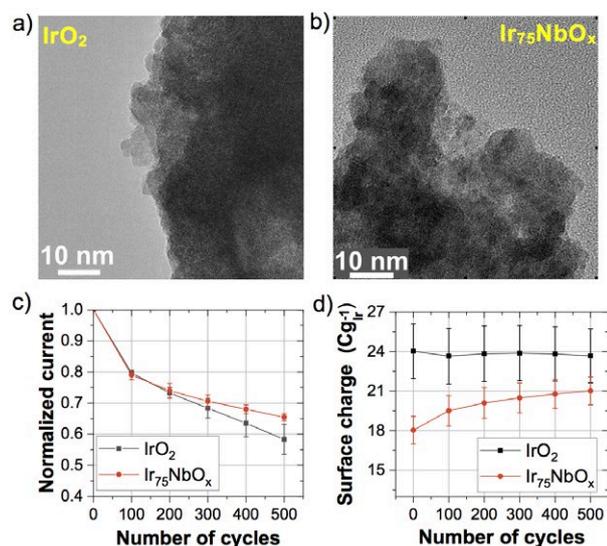
Figure 2. HRTEM images of IrO_2 (a) and IrN_bO_x, 75 wt% Ir (b); normalized current at 1.6 V during a stability accelerated stress test protocol (potential steps between 1.0 V and 1.6 V vs RHE, holding 10 s at each potential, in 0.1 M $HClO_4$ at room temperature) in an RDE setup, (c) and integrated surface charge as a function of the number of cycles (d).

Ionic contamination of catalyst coated membranes

Degradation vectors of PEWE yield a complex matrix of interconnected parameters which determine final durability and lifetime of the device [4–7] but there is one factor which stands out, because it is mostly end user driven. Solid electrolyte membrane water electrolyzers are very sensitive to the presence of ionic contaminants in the feed water. On the one hand, they originate from system components, such as piping, PTLs, heat exchangers, etc. On the other hand, the feed water may not be sufficiently deionized. Ultra-pure water supply is crucial for the stable and long-term operation of the membrane electrolyzer [8–10]. Purification of the water is usually realized by installation of an ion exchanger in the loop, but even then small amounts of impurities will reach the CCM and accumulate over time, finally leading to considerable performance loss. It is therefore important to develop a strategy and techniques to either mitigate ionic contamination or introduce regeneration procedures.

Recent efforts have shown that the contaminants accumulate in the vicinity of the cathode catalyst layer under the effect of the electric field [9]. Localized high concentration is a favorable situation for *in situ* regeneration, since the rate of ion removal will scale with the concentration gradient. As a result, a novel approach to CCM regeneration was established, whereby only the cathode compartment of the cell is used. In order to remove the ionic contaminants from the CCM, one needs to provide a counter ion to which the contaminant can associate in exchange for a proton. The most common regenerating or protonating medium used *ex situ* is sulfuric acid but, due to its corrosive influence on the system components, e.g. piping, flow meters, valves etc., the technical feasibility of such a solution in a working system is limited. In our approach, the regeneration process has been redesigned in a way that the acidic medium is no longer delivered from the outside through the pipework but will be generated within the cell by saturating the water already present on the cathode side with CO_2 gas, which will lead to carbonic acid formation [11]:

$$H_2O + CO_2 \leftrightarrows H_2CO_3$$
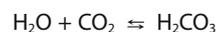
Figure 3 presents the voltage profile over time obtained during a contamination / regeneration experiment. The regeneration was performed at the pressure of 21 bar in order to achieve a pH of circa 3 in the cathode compartment. The baseline and final regenerated curve are at ambient conditions. The cell was almost fully regenerated after a period of 20 h. What has to be highlighted is that the cell was severely contaminated. Such level would probably never be seen in industrial stacks and regeneration action would be taken much earlier. The regeneration would then take significantly longer in such a case since the concentration of the contaminants in the catalyst layer would be much lower and therefore one should expect a slower ion exchange process. This phenomenon can also be seen while analysing Figure 3: one can observe that the regeneration rate decreases at longer times.
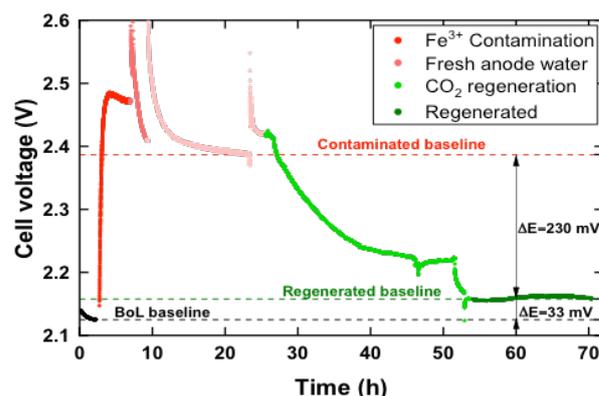
Figure 3. Voltage profile of the contamination experiment followed by the regeneration procedure using CO_2 at a constant current density of 1 A/cm^2. Cell temperature was ~40°C, determined by heat generation in the cell due to losses (no external heating). The pressure under which the regeneration was performed was 21 bar.

The proof of concept of the new regenerating method was successful but, in order to make it application-ready, there is still much work to be done. The study will be expanded by a

parametric study including current density impact on regeneration rate, ways of introducing CO_2 to the system, and most effective formation of carbonic acid (either in the water/gas separator or in the cell itself).

On the role of microporous transport layers for high performance PEWE cells

Porous transport layers are one of the key components for polymer electrolyte water electrolysis. The impact of PTL microstructure on overpotentials has been a question of dispute in literature so far. Conventionally, bulk properties were compared to electrochemical performance and mass transport losses considered to originate from the bulk microstructure of the PTLs.

Recent studies revealed that the interface between catalyst layer and PTLs is the more important governing design parameter for high cell efficiency [12, 13]. With conventional porous transport layers, partial catalyst layer utilization may lead to high kinetic and mass transport overpotentials. State-of-the-art PTLs do not meet the requirements of a highly efficient microstructural design. For high mechanical integrity and high open porosity, today economically viable bulky Ti powder materials are used as the feedstock for PTLs resulting in PTL structures with high surface roughness and low surface area.

A novel approach of hierarchically structured PTLs is therefore pursued. Finer titanium powders fill the abyssal valleys at the surface of single-layer PTLs and result in high surface area. A generic structure of a multi-layered PTL is shown in a 3D X-ray tomographic microscopy rendering, in Figure 4. The fine top-layer consists of low-cost irregular shaped titanium particles and is merged to a coarse support layer through a co-sintering process.
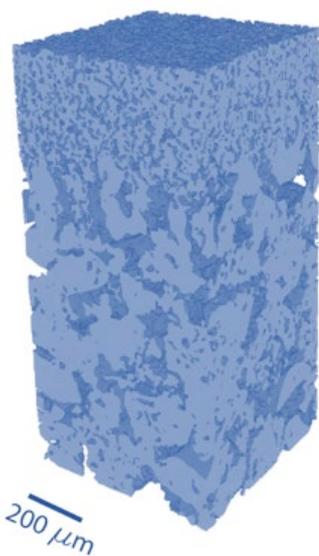
Figure 4. 3D XTM rendering of a generic multilayer PTL dry structure.

The advantage of a microporous layer becomes obvious when comparing the electrochemical performance of a support-layer-only material, featuring comparable surface and bulk properties as commercially available sintered materials, to a PTL with an additional microporous layer. From the low cur-

rent density regime of up to 100 mA/cm^2, dominated by OER kinetics induced overpotentials, to the high current density regime at 4 A/cm^2, dominated by ohmic and mass transport losses, the single layer material is clearly outperformed. As shown in Figure 5, at the industrially relevant current density of 2 A/cm^2, the microporous layer-PTL reduces the overpotential by 120 mV.

The engineering of the electrochemical interface between catalyst layer and PTL surface is the key to next generation high performance PTL materials. More details are given in ref. [14].
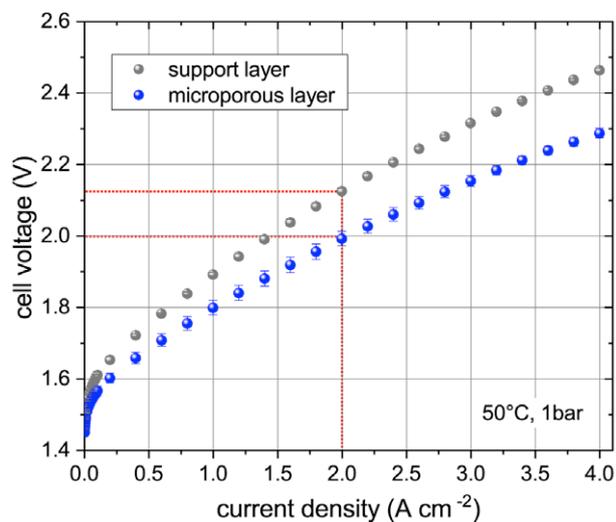
Figure 5. Polarization curves of single-layer-only PTL and microporous layer PTL with commercial CCMs based on Nafion 115 (Greenerity E400, Germany) at 50°C and 1 bar$_a$.

Hydrogen crossover suppression

A key concern for the safe operation of polymer electrolyte water electrolysis (PEWE) cells is the high hydrogen gas crossover that can lead to explosive hydrogen-oxygen gas mixtures. The lower limit of explosion is at 4% hydrogen in oxygen. Commercial electrolysers are operated at about 60°C, 30 bar differential pressure, and with membranes of 200 µm thickness [6]. The safety aspect is especially important with thinner membranes and high differential pressures. Impregnating Pt particles into the membrane results in the recombination of hydrogen and oxygen on the catalyst's surface during PEWE operation [15]:

$$H_2 + \tfrac{1}{2}O_2 \rightarrow H_2O$$
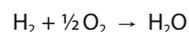
In our concept Pt-ions are exchanged into a Nafion NR212 proton exchange membrane (PEM) with a nominal thickness of 60 µm using a Pt-ion containing solution. In a second step the ions are reduced by hydrogen permeating through the membrane yielding Pt particles with a diameter of around 10 nm and a platinum content of 0.1 mg cm^{-2} [16].

Figure 6 shows the behavior of a pristine Nafion NR212 membrane and of a Pt doped Nafion NR212 membrane between 0.5 and 2 A/cm^2 electrolysis operation. The result shows a decreasing hydrogen fraction with increasing current density as the rate of the oxygen evolution reaction is increasing [17]. In comparison to pristine NR212, the hydrogen content was significantly reduced for the Pt-N212 membrane over the whole current density range [18].
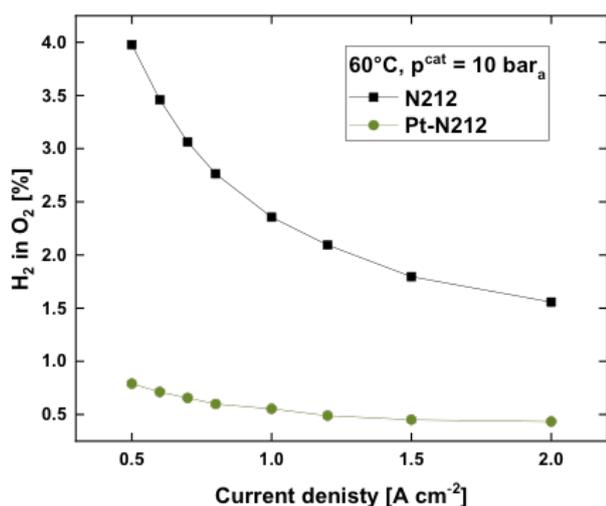
Figure 6. *Content of hydrogen in oxygen at 10 bar$_a$, 5 bar$_a$, and 10 bar$_a$ cathodic pressure, respectively, and 60°C for a PEWE cell using pristine NR212 (N212, black) and a PEWE cell using a Pt doped NR212 obtained by reduction with hydrogen (Pt-N212, green).*

Future experiments are targeting to investigate the reduction of platinum loading and its impact on cross-over suppression.

Conclusion

New materials for PEWE cells contribute to improving the efficiency of hydrogen production. OER catalysts with higher specific surface area allow a reduction of the catalyst loading on the anode. Also, catalysts with higher stability improve the lifetime of PEWE cells.

Thin membranes are essential to reducing ohmic losses, in particular when higher current densities of 4–6 A/cm^2 are targeted. This calls for strategies to mitigate gas crossover. The approach shown here is based on the incorporation of a H_2-O_2 recombination catalyst.

Furthermore, the interface between PTL and catalyst-coated membrane needs to be adequately designed to prevent membrane creep, failure, and to maximize catalyst utilization. Our unique approach consists of a graded titanium sinter material with smooth surface facing the membrane.

The most common failure of PEWE systems in the field is related to cationic contamination of the ionomer. Our approach for decontamination using CO_2 could be used in an operating system without time consuming and resource intensive maintenance operation.

Contact

For further information, please contact Dr. Pierre Boillat, Dr. F.N. Büchi, PD Dr. Lorenz Gubler, or Prof. T.J. Schmidt:

pierre.boillat@psi.ch
felix.buechi@psi.ch
lorenz.gubler@psi.ch
thomasjustus.schmidt@psi.ch

Contributors

The contributors for this particular research topic are N. Diklic, S. Garbe, T. Schuler, and M. Zlobinski.

Acknowledgement

References

[1] E. Fabbri, A. Habereder, K. Waltar, R. Kötz, T.J. Schmidt, *Catal. Sci. Technol.* **4**, 3800–3821 (2014).

[2] J. Herranz, J. Durst, E. Fabbri, A. Pătru, X. Cheng, A.A. Permyakova, T.J. Schmidt, *Nano Energy* **29**, 4–28 (2016).

[3] M. Povia, D.F. Abbott, J. Herranz, A. Heinritz, D. Lebedev, B.-J. Kim, E. Fabbri, A. Pătru, J. Kohlbrecher, R. Schäublin, M. Nachtegaal, C. Copéret, T.J. Schmidt, *Energy Environ. Sci.* **12**, 3038–3052 (2019).

[4] M. Carmo, D.L. Fritz, J. Mergel, D. Stolten, *Int. J. of Hydrogen Energy* **38**, 4901–4934 (2013).

[5] C. Rakousky, U. Reimer, K. Wippermann, M. Carmo, W. Lueke, D. Stolten, *J. Power Sources* **326**, 120–128 (2016).

[6] U. Babic, M. Suermann, F.N. Büchi, L. Gubler, T.J. Schmidt, *J. Electrochem. Soc.* **164**, F387–F399 (2017).

[7] S. Sun, Z. Shao, H. Yu, G. Li, B. Yi, *J. Power Sources* **267**, 515–520 (2014).

[8] X. Wang, L. Zhang, G. Li, G. Zhang, Z.-G. Shao, B. Yi, *Electrochim. Acta* **158**, 253–257 (2015).

[9] U. Babic, M. Zlobinski, T.J. Schmidt, P. Boillat, L. Gubler, *J. Electrochem. Soc.* **166**, F610–F619 (2019).

[10] L. Zhang, X. Jie, Z.-G. Shao, X. Wang, B. Yi, *J. Power Sources* **241**, 341–348 (2013).

[11] U. Babic, M. Zlobinski, P. Boillat, L. Gubler, European Patent Application No. 18196579.9 , Paul Scherrer Institut (2018).

[12] T. Schuler, R.D. Bruycker, T.J. Schmidt, F.N. Büchi, *J. Electrochem. Soc.* **166**, F270–F281 (2019).

[13] T. Schuler, T.J. Schmidt, F.N. Büchi, *J. Electrochem. Soc.* **166**, F555–F565 (2019).

[14] T. Schuler, J.M. Ciccone, B. Krentscher, F. Marone, C. Peter, T.J. Schmidt, F.N. Büchi, *Adv. Energy Mater.* **10** (2), 2070009 (2020).

[15] S.A. Grigoriev, P. Millet, S.V. Korobtsev, V.I. Porembskiy, M. Pepic, C. Etievant, C. Puyenchet, V.N. Fateev, *I. J. Hydrogen Energy* **34**, 5986–5991 (2009).

[16] S. Garbe, U. Babic, L. Gubler, T.J. Schmidt, European Patent Application No. EP19175071.0, Paul Scherrer Institut (2019).

[17] P. Trinke, B. Bensmann, R. Hanke-Rauschenbach, *Int. J. Hydrogen Energy* **42**, 14355–14366 (2017).

[18] S. Garbe, U. Babic, E. Nilsson, T.J. Schmidt, L. Gubler, J. Electrochem. Soc. 166, F873-F875 (2019).

Evaporative cooling of polymer electrolyte fuel cells

Even though state-of-the-art polymer electrolyte fuel cells (PEFC) reach system efficiencies above 60 %, a substantial amount of heat has to be rejected to the environment. Conventional cooling approaches aim at transferring the waste heat to a liquid coolant that flows through dedicated cooling channels. This yields high heat fluxes from the cell to the coolant and ensures a uniform temperature distribution but requires a thick and complex design of bipolar plates. As a novel concept, evaporative cooling does not require separate cooling channels and is therefore capable to reduce the fuel cell system volume, complexity and cost by up to 30 %. Additionally, the water evaporates close to the membrane and therefore contributes to a better humidification and thus higher ionic conductivity, which enables higher operating temperatures without the need for external humidification.

The operating temperature of polymer electrolyte fuel cells (PEFC) is mainly limited by the ionic conductivity of the proton exchange membrane, which is highly affected by the relative humidity in the gas channels [1]. As a consequence, state of the art PEFCs are typically operated in a temperature range of 60°C to 80°C. To keep the operating temperature within this range, conventional approaches aim to remove the waste heat by convective heat transfer to a liquid coolant through separate cooling channels in the bipolar plates. This yields high heat fluxes from the cell to the coolant and ensures a uniform temperature distribution but requires a thick and complex multi-layer design of bipolar plates [2]. Consequently, the heated coolant is chilled in an external heat exchanger, which typically requires a high surface area due to the small temperature difference to the environment.

One promising approach to overcome these obstacles is evaporative cooling. Liquid water is introduced into a specially designed carbon-fibre gas diffusion layer (GDL) with patterned wettability through a dedicated water channel in the flow field (see Figure 1) [3]. The water consequently evaporates which cools the cell and simultaneously contributes to a better membrane humidification. Additionally, evaporative cooling shows the potential to reduce the system volume, mass, complexity and cost by simplifying the design of bipolar plates and balance of plant [4]. However, the interactions between operating conditions, evaporation, electrochemistry and system volume are complex.
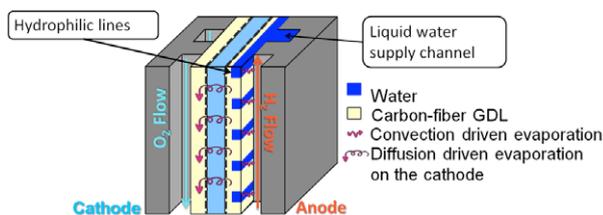
Figure 1. *Schematic representation of an evaporatively cooled PEFC [3].*

Copyright © 2018 by John Wiley & Sons, Inc. Reprinted by permission of John Wiley & Sons, Inc.

This report focuses on three aspects of evaporative cooling. In the first part, a zero-dimensional fuel cell system model is presented and suitable operating conditions for evaporative cooling are elaborated. The second part covers the development and testing of gas diffusion layers with patterned wettability. Finally, part three presents experimental results of a differential fuel cell operated with evaporative cooling and discusses the effects of evaporative cooling on membrane humidification.

Zero dimensional fuel cell system model and simulation results

In order to quantify the potentials and limits of the evaporative cooling approach, a semi-empirical zero-dimensional fuel cell system model has been developed. Each system component (e.g. stack, compressor, condenser, etc.) is modeled zero-dimensionally and is therefore considered as a black box. Hence, only the fluxes across the system boundaries as well as sink and source terms are taken into account to model mass and energy balance. For the stack, electrochemical equations (i.e. Nernst potential, kinetics, ohmic losses and mass transport losses) are additionally considered. Relevant electrochemical parameters and evaporation rates have been determined experimentally from an actual evaporatively cooled differential fuel cell with an active area of 4.4 cm^2 [3]. The outlet of each model component is connected to the inlet of the subsequent one. That finally yields a system of coupled ordinary differential equations. The solution delivers the thermodynamic state at each position in the considered domain as well as the electrochemical performance of the stack.

First, the zero dimensional fuel cell system model was applied to study the impact of different operating conditions (i.e. temperature, pressure and stoichiometry) on the maximum possible evaporation rate and thus cooling performance. Main findings show that an increased operating temperature and stoichiometry as well as a decreased system pressure are increasing the evaporation rate and are therefore beneficial for the cooling performance (see Figure 2).
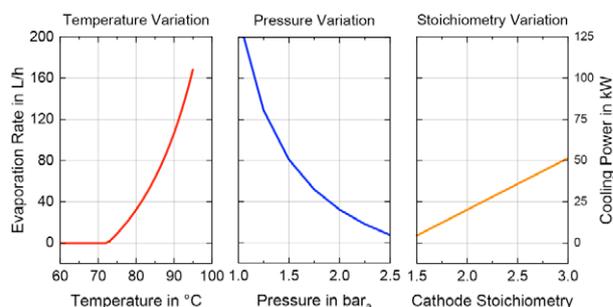
Figure 2. *Simulated evaporation rates and cooling power as a function of operating temperature, pressure and cathode stoichiometry for a 100 kW$_p$ stack operated at 1.5 A/cm^2.*

The fuel cell system shows an isothermal behaviour if the waste heat is equal to the heat of evaporation (i.e. thermal neutrality).
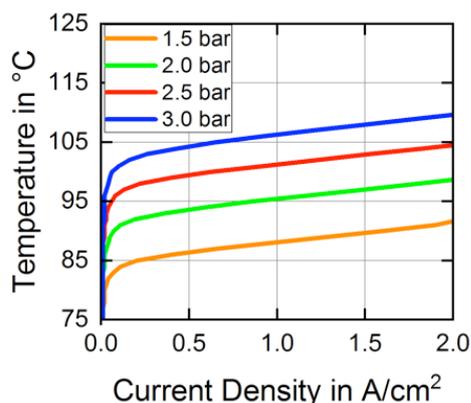
Figure 3. *Simulation results of steady state fuel cell temperature as a function of system pressure and current density at a stoichiometry of 2.0 at the cathode and 1.5 at the anode.*

Since both parameters depend on the actual operating conditions and system load, it can be shown that the steady-state temperature is a function of system pressure, stoichiometry and current density (see Figure 3).

Second, the impact of operating conditions on the electrochemical performance has been studied. Simulation results show that the performance is slightly decreased (-25 mV at 1 A/cm^2) at operating conditions which are favourable for evaporative cooling (1.5 bar, dry gases), in comparison to conventional operating conditions (2 bar, 80°C, fully humidified gases). Additionally, an earlier mass transport limitation can be observed, which is mainly affected by the lower oxygen partial pressure at 1.5 bar (see Figure 4).
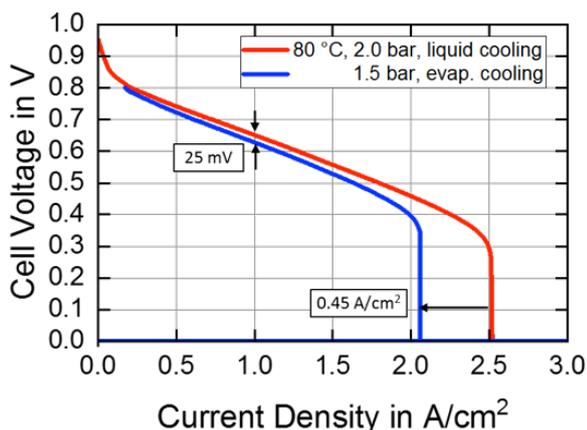
Figure 4. *Comparison of simulated electrochemical performance of a conventional fuel cell (red) at 80°C and 2 bar with an evaporatively cooled cell (blue) at 1.5 bar.*

Third, the water balance of an evaporatively cooled fuel cell system has been investigated to proof that a sufficient amount of water can be condensed from the exhaust gas and no additional water supply is necessary. It could be shown that a closed water loop is possible at condenser outlet temperatures below 60°C. That means, a sufficient amount of water can be retained from the exhaust gas and be refed to the stack in order to ensure a satisfactory cooling performance over a broad range of operating conditions (see Figure 5).

Based on the simulation results, a feasible operating window for evaporative cooling can be proposed which is shifted towards higher temperatures (approx. 85°C to 100°C) and slightly lower pressures (approx. 1.5 to 2.5 bar) compared to conventional fuel cell systems.
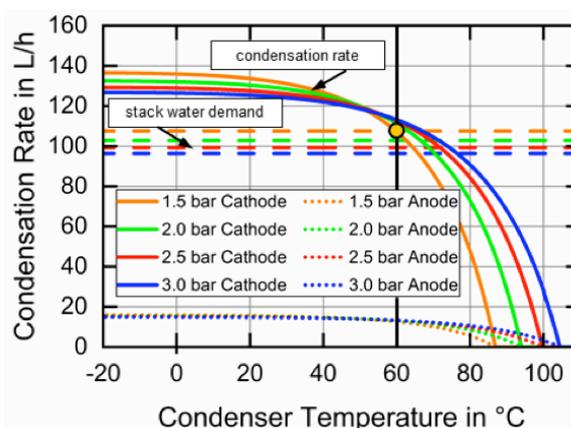
Figure 5. *Calculated exhaust gas condensation rates at cathode (solid lines) and anode (dotted lines) as well as stack water demand for evaporative cooling (dashed lines) as a function of condenser outlet temperature and operating pressure.*

Gas diffusion layer development and testing

To enable the evaporative cooling concept, a specially modified GDL is used. The GDL is made hydrophobic by coating the porous material with a fluoropolymer layer, a practice commonly implemented for commercially available GDLs. Later, certain regions of the coating are turned hydrophilic by selectively performing radiation induced grafting polymerization. The resulting GDL incorporates hydrophilic regions perpendicular to the water channels to act as water distributors (see Figure 6). The hydrophilic regions present in the GDL need to distribute the water through the entire GDL at least at the same rate as it evaporates.
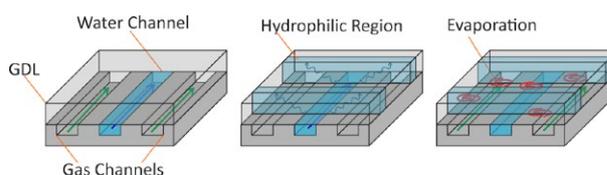
Figure 6. *Sketch of the application of GDLs with patterned wettability in evaporative cooling [5].*

The water injection by capillary pressure from a channel to the GDL optimizes the water separation in the patterned GDL since the water intrudes the GDL through the pathway with less capillary pressure, which are the hydrophilic regions. Thanks to the water channel providing hydraulic connection, the hydrophobic regions remain dry. The effects of different material modifications, such as coating load and substrate type on the wetting dynamics of the GDLs were investigated experimentally.

The water imbibition dynamics were tested by recording the time a water droplet on the surface of the GDL requires to be absorbed by the material. The measurements were performed placing a water drop of 3 µL on the surface and the initial volume of the drop was compared with the remaining volume at each time frame. For this measurements hardware and soft-

ware OCA 25 Dataphysics were employed. This technique and the results on the effect of coating load have being previously published [6] and are repeated here for comparison.
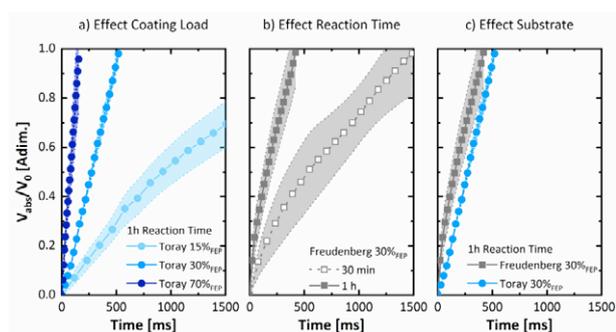
Figure 7. *Wetting dynamics for different hydrophilic substrates, comparing the effect of (a) coating load [6], (b) reaction time and (c) substrate type. The error bars represent the standard error of the average of 5 different measurements.*

This test is used to screen suitable parameters for modification of GDLs. Only the materials with fastest absorption dynamics have shown adequate performances during evaporation tests. Figure 7 shows the effect on wetting dynamics when comparing three different parameters. Regarding the coating load (Figure 7-a) the highest coating load shows the fastest absorption dynamics. The high coating load ensures that a large percentage of the fibres are covered by coating material and therefore upon grafting the majority of the surface in the modified region is hydrophilic.

The reaction time of the grafting polymerization (Figure 7-b) is also a key parameter to consider. Although the studies in films show that similar amounts of grafting and contact angles are reached between reaction times of 30 minutes and 1 hour (see our previous publication [6]), the absorption dynamics differ. This is probably due to the porosity of the GDL, which hinders the transport of the reactant monomer.

The last tested parameter was the substrate type (Figure 7-c). Under the same conditions, the Freudenberg GDL shows faster wetting dynamics, however the irreproducibility of the measurement is higher than for the Toray GDL. Although promising, when the Freudenberg GDLs with high coating loads were tested for evaporation, no spontaneous wicking of water was observed. Our hypothesis is that, due to the narrower pore size distribution of the Freudenberg GDL, the high coating loads in this type of GDLs reduce the porosity to a degree where the material is no longer wicking the water – unlike what happens with the Toray material. The Toray GDL have shown adequate behaviour in terms of water imbibition and evaporation when the materials were heavily coated using up to 70 % FEP coating load, in order to ensure spontaneous wicking of water in the material [7].

Experimental investigation of evaporative cooling in differential single cells

Humidification of the membrane is one of the most critical aspects of PEFCs. Without a proper humidification, a fuel cell will have strongly degraded performance and will fail at much lower current density than with humidification [8–10]. It was therefore extremely important to prove that the PSI evaporative cooling concept can actually achieve adequate levels of humidification.

An experimental test cell has been built to study our evaporative cooling concept. In addition to the measurement of voltage and current, it allows very precise and fast temperature regulations thanks to Peltier elements and heat flux sensors that can help to determine the net amount of heat consumed or rejected by the cell. Last, it is built with materials transparent enough to neutrons to allow the detection of small amounts of water even behind such complex instrumentation as neutron radiography (NR) [4, 11]. It must be noted that our test cell is a differential cell, i.e. a small active area cell (4.4 cm^2), operated with very high stoichiometries. While this operation mode is very favourable for evaporating water, it is not favourable for the humidification of the gases.

The level of humidification of the membrane is typically characterised by the high frequency resistivity (HFR), i.e. the real part of the impedance at frequencies above 10 kHz multiplied by the surface area of the cell. A typical value for the state-of-the-art Gore Primea 517 membrane that is used in our test cell is 40 mΩ cm^2 at full humidification (100 % relative humidity on both sides) [12].

In our concept, the evaporation takes place on the anode and is driven in large part at first by the convection due to the anode gas flow. As usual with convection-driven transport phenomena, a very important parameter is the contact surface between the two phases, i.e. the water in the hydrophilic lines and the anode gas flow. In order to determine how efficient our scheme is at humidifying the reactant gases, we needed to determine how the HFR would evolve. Therefore, a neutron radiography experiment was conducted at the ICON beamline at the Swiss spallation source SINQ at Paul Scherrer Institute. As explained before, NR allows the detection of water behind dense materials: here it helped seeing the water in the hydrophilic lines and in the water supply channel. The contact surface between the water in the hydrophilic lines and the gas flow could then be extracted from these images thanks to a post-processing program, based on Otsu's algorithm, for the automatic detecting of thresholds [3]. In order to change the contact surface in this experiment, the mass flow rate of liquid supplied to the water channel on the anode is varied between 2 and 8 g/hr. Since these values are lower than the maximal possible evaporation rate at these temperature and pressure, the water front in the supply channel was not able to reach the end of the test cell. Instead, it could only provide water to a limited number of hydrophilic lines, meaning that the contact surface between the water in the hydrophilic lines and the anode gas flow would change depending on the liquid flow rate, as shown by the post-processed NR images in Figure 8.
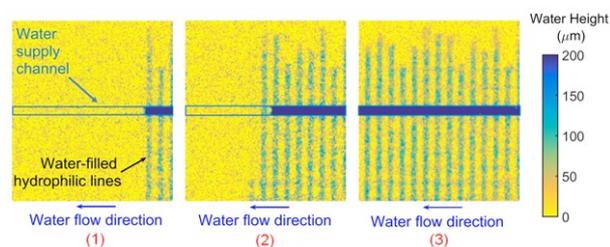
Figure 8. *Neutron Radiography images of the fuel cell with evaporative cooling concept. Water is supplied in the water supply channel at different mass flow rates: 2 g/hr (1), 5 g/hr (2) and 8 g/hr (3).*

The resistivity measured for each point is plotted in Figure 9 against the contact surface measured by the procedure described previously. As expected, once the contact surface increases, so does the relative humidity, and the resistivity de-

creases sharply. Most important, for a contact surface as small as 80 mm², the resistivity is already around 60 mΩ cm², very close to the optimal value measured on this state-of-the-art membrane for full humidity on both sides.
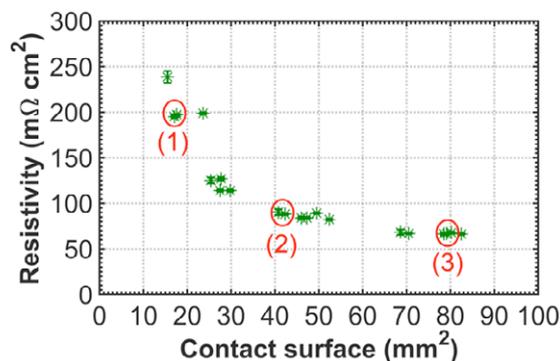
Figure 9. *Resistivity versus contact surface determined by neutron radiography.*

In a non-operating cell, evaporation takes place on the anode and the vapour is removed either on the anode or on the cathode. On the anode side, the vaporization process is dominated by the convection of the anode flow, whereas on the cathode side it is dominated by the diffusion of the vapour from the hydrophilic lines to the cathode gas channels through all the various layers of the cell.

A one-dimensional (1-D) model was developed to predict evaporation in the fuel cell in non-operating conditions [3]. This model shows how the evaporation rate and the cooling power are function of the temperature, the pressure, the anode and cathode mass flow rates and the contact surface between the water in the hydrophilic lines and the anode gas flow. This model was tested and fitted against the anode and cathode mass flow rates for a temperature of 80° C and 2 bar. Using the same experiment described above, the 1-D model was compared to the total measured heat flux due to vapourisation as a function of the contact surface (Figure 10). The 1-D model is in fairly good agreement with the experimental results.
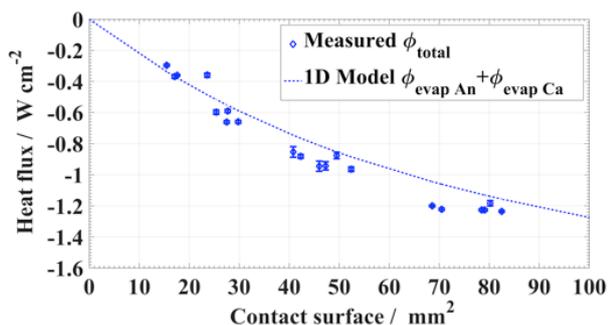
Figure 10. *Evolution of the total heat flux due to evaporation in a non-operating cell versus the contact surface between water and anode gas flow. Comparison between the 1-D model and the experimental results.*

Copyright © 2018 by John Wiley & Sons, Inc. Reprinted by permission of John Wiley & Sons, Inc.

Based on the experimental results it can be shown that the geometry of the hydrophilic lines and their distribution are important parameters, since they control the contact surface. While the temperature and pressure control the maximal possible evaporation rate and thus the maximal cooling power, they do not control the local relative humidity increase, which is only controlled by the mass flow rates on the anode and the cathode and the contact surface between water and gas flow.

Conclusion

It has been shown that evaporative cooling is a promising alternative to conventional cooling concepts for PEFC. A zero-dimensional fuel cell system model has been developed and simulation results show that sufficient cooling power can be provided at slightly changed operating conditions, compared to conventional operation. Furthermore, the electrochemical performance is only slightly affected. Next, it has been shown that GDLs with patterned wettability, produced by radiation grafting, are capable to spontaneously wick water and distribute it sufficiently fast across the cell. Finally, a neutron imaging study has been conducted and experiments have proven that the PSI evaporative cooling approach contributes to a better membrane humidification without the need for external humidification.

Contact

For further information on porous materials for fuel cells or electrolysers, please contact Dr. Pierre Boillat, head of the *Neutron Radiography of Electrochemical Systems* group or Dr. Felix Büchi, head of the *Fuel Cell Systems and Diagnostics* group.

pierre.boillat@psi.ch
felix.buechi@psi.ch

Contributors

The contributors for this particular research topic are M. Striednig, M. Cochet, V. Manzi-Orezzoli, D. Scheuble, T.J. Schmidt, P. Boillat and F.N. Büchi.

Acknowledgement

References

[1] A. Kusoglu, A.Z. Weber, *Chem. Rev.* **117**, 987 (2017).
[2] G. Zhang, S.G. Kandlikar, *Int. J. Hydrogen Energy* **37**, 2412 (2012).
[3] M. Cochet, A. Forner-Cuenca, V. Manzi-Orezzoli, M. Siegwart, D. Scheuble, P. Boillat, *Fuel Cells* **18** (5), 619 (2018).
[4] A. Fly, R.H. Thring, *Int. J. Hydrogen Energy* **41**, 14217 (2016).
[5] V. Manzi-Orezzoli, PhD thesis, No. 26404, ETH Zürich (2019).
[6] A. Forner-Cuenca, V. Manzi-Orezzoli, J. Biesdorf, M. El Kazzi, D. Streich, L. Gubler, T.J. Schmidt, P. Boillat, *J. Electrochem. Soc.* **163**, F788 (2016).
[7] A. Forner-Cuenca, J. Biesdorf, A. Lamibrac, V. Manzi-Orezzoli, F.N. Büchi, L. Gubler, T.J. Schmidt, P. Boillat, *J. Electrochem. Soc.* **163**, F1038 (2016).
[8] A.V. Anantaraman, C.L. Gardner, *J. Electrochem. Soc.* **414**, 115 (1996).
[9] F.N. Büchi, S. Srinivasan, *J. Electrochem. Soc.* **144**, 2767 (1997).
[10] J. Zhang, Y. Tang, C. Song, X. Chen, J. Zhang, H. Wang, *Electrochim. Acta* **52**, 5095 (2007).
[11] P. Boillat, E.H. Lehmann, P. Trtik, M. Cochet, *Curr. Opin. Electrochem.* **5**, 3 (2017).
[12] P. Oberholzer, P. Boillat, *J. Electrochem. Soc.* **161**, F139 (2014).

How X-ray absorption, emission and Mössbauer spectroscopies can help to unravel the composition of Fe-based electrocatalysts

Iron-based catalysts have displayed promising initial activities for the electroreduction of O_2 and CO_2, but their performance and stability remain insufficient for their implementation in fuel cell or co-electrolyzer cathodes. Improving these key features requires a better understanding of the structure and electronic properties of these catalysts' active sites, consisting of N-coordinated Fe-atoms embedded in a carbon backbone. In this contribution, we show how X-ray absorption and emission spectroscopies (two techniques available at the SuperXAS beamline of the Swiss Light Source) complemented by Mössbauer spectroscopy can help to shed light on these crucial features

The extended implementation of renewable energy sources could be jeopardized by their intrinsic intermittency, which calls for a wider diversification of energy storage and conversion technologies. Among the latter, (co-)electrolysers use renewable electricity to produce added-value carbon compounds (e.g., formic acid) through the reduction of CO_2, or to directly produce H_2 from water [1]. In the latter case, the hydrogen could be subsequently re-electrified in so-called polymer electrolyte fuel cells (PEFCs), which are well suited for the propulsion of electric vehicles with an extended driving range ($\approx$ 500 km per fuelling operation).

Chiefly, the successful implementation of these energy conversion devices strongly relies on the development of highly active, stable and selective catalysts for the reactions at play in their electrodes; among these, CO_2- and O_2-electroreduction are widely regarded as the major bottlenecks for co-electrolyser and PEFC development, respectively [1–3]. On top of these requirements, such electrocatalysts should rely on affordable and abundant materials, as to minimize their impact on the devices' cost and long-term applicability – a key prerequisite that is not fulfilled by the noble-metal catalysts implemented in state-of-the-art PEFCs and electrolysers [3].

To tackle these needs, an extensive amount of work is currently being devoted to the development of catalysts based on transition metals like Fe or Co, which in recent years have been shown to display very promising initial performances for the reduction of O_2 or CO_2 [4, 5]. Despite this progress, further improvements in their activity and stability are urgently required, and have translated in an ongoing effort to establish relations between these catalytic properties and the materials' composition [6, 7].

For the Fe-based catalysts that generally display the best performance among these materials (referred to as Fe/N/Cs in what follows), Mössbauer spectroscopy (MS) has revealed extremely helpful for such catalyst speciation studies. In particular, this technique allows differentiating among Fe-based particles (e.g., iron carbides) often present in such materials and the atomically dispersed and N-coordinated iron sites (Fe-N$_x$) depicted in Figure 1, which have been extensively related to their O_2-reduction reaction (ORR-) activity [6]. These Fe-N$_x$ centers have been assigned to Mössbauer doublets with spectroscopic parameters (i.e., isomer shift and quadrupole splitting) similar to those displayed by structurally simpler, N-coordinated Fe-compounds (e.g., porphyrins). While these similarities have sometimes been used to ascribe a structural configuration, oxidation and spin state to these doublets and corresponding Fe-N$_x$ sites, this assignment remains highly

tentative and should be verified with complementary techniques capable of assessing these properties [8, 9]. Moreover, the combination of MS's exclusive sensitivity to ^{57}Fe with the low metal content characteristic of these catalysts (typically < 5 wt.% Fe) translates in the need to synthesize the materials of interest using ^{57}Fe precursors; however, the effect of this common practice on the resulting materials' catalytic and compositional features is also unknown.
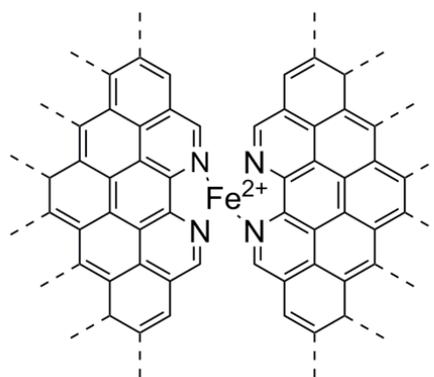
Figure 1. Proposed structure of the atomically dispersed sites in Fe/N/C-catalysts [6], whereby an iron ion is coordinated by N-moieties embedded in opposite graphene platelets.

With these motivations, in the first part of this contribution we report our efforts at using X-ray absorption spectroscopy (XAS) in combination with MS to determine how ^{57}Fe-enrichment affects the composition of a series of Fe/N/C-catalysts. Subsequently, the second section presents our first results using X-ray emission spectroscopy (XES) to quantify the average spin state of such catalysts, in a first step to precisely assign the spin states of these Fe-N$_x$ centers.

^{57}Fe-enrichment effect on activity and composition

A series of Fe/N/C-catalysts with similar overall iron contents ($\approx$ 1.0–1.5 wt.% Fe) but with ^{57}Fe-enrichment extents from 0 to 100 % (i.e., exclusively containing ^{56}Fe or featuring 25, 50 or 100 % ^{57}Fe) were prepared using the synthesis procedure developed by Ebner et al. [10]. As displayed in Figure 2a, increasing the fraction of ^{57}Fe from 0 to 100 % of the overall iron content led to a $\approx$ 4 fold decrease of the catalysts' ORR activity that, to the best of our knowledge, has never been previously reported.

Upon MS characterization of the three ^{57}Fe-containing samples, their spectra displayed three doublets that have been previously assigned to Fe-N$_x$ sites, along with a singlet and two sextets related to superparamagnetic iron, Fe$_3$C and α-Fe, respectively (see Figure 2b for an exemplary spectrum of the 25 % ^{57}Fe-enriched catalyst). Most importantly, the partial content of the Fe-N$_x$-related doublets decreases with the catalysts' ^{57}Fe-enrichment extent (see Figure 3b), in agreement with the established relation between these atomically dispersed sites and the materials' ORR-activity [6]. On the other hand, a direct correlation between ORR-activity and this MS-inferred Fe-speciation may be misleading, since it excludes the non ^{57}Fe-enriched catalyst (which displays the best performance) and suffers from MS's exclusive sensitivity to ^{57}Fe. Specifically, if the speciation of the ^{56}Fe and ^{57}Fe atoms in the partially ^{57}Fe-enriched samples were to be different, MS would only capture the ^{57}Fe phases and thus provide a biased picture of this crucial feature and its relation to the ORR-activity.

and Fe-N$_x$ sites [7] at the origin of the main sextet and three doublets in Figure 2b, respectively.

As displayed in Figure 3b, the sample's Fe-N$_x$ sites content derived from this fitting approach ($\approx$ 60 %) excellently agrees with the combined fraction of the three Mössbauer doublets assigned to such sites. This good agreement among the quantitative results obtained with the two techniques extends to the 100 % ^{57}Fe enriched sample, but somehow larger deviations are observed for the catalyst containing 50 % ^{57}Fe. According to the MS results, this catalyst features a larger amount of superparamagnetic iron that is not considered in the LCF of its XANES spectrum and that possibly causes this slight inconsistency. Beyond this imprecision, the good match among XAS and MS results indicates that the speciation of the iron in these catalysts is the same for their ^{56}Fe and ^{57}Fe atoms, and that the MS-results are fully representative of the compositional distribution of the iron in these samples.

Figure 2. *Effect of the Fe/N/C-catalysts' ^{57}Fe-enrichment extent on their corresponding ORR-activity, expressed as the mass-normalized kinetic current at an iR-corrected potential of 0.8 V vs. the reversible hydrogen electrode ($i_{kin,iR-corrected}$), as inferred from rotating disc electrode measurements in O$_2$-saturated 0.1 M HClO$_4$ (a). Exemplary, deconvoluted Mössbauer spectrum of the 25 % ^{57}Fe-enriched catalyst (b).*

To verify this possibility, an alternative technique with equal sensitivity to both Fe-isotopes is needed. This requirement is fulfilled by XAS, whereby the X-ray absorption near edge structure (XANES) spectrum in the vicinity of the absorption step is highly sensitive to a given analyte's oxidation state. The absorbate's composition can then be estimated through a linear combination fit (LCF) of the acquired XANES spectrum based on the reference spectra of its known components. This approach is illustrated in Figure 3a, which displays the XANES spectrum of the 25 % ^{57}Fe-enriched catalyst, along with the LCF spectrum obtained using reference spectra for the Fe$_3$C

Figure 3. *Fe K-edge XANES spectrum of the catalyst with 25 % ^{57}Fe-enrichment, along with the result of its linear combination fit (LCF) within the energy region indicated by the vertical grey lines based on the reference spectra of Fe-N$_x$ sites (from Ref. 7) and Fe$_3$C (a). Effect of the catalysts' ^{57}Fe enrichment extent on their Fe-N$_x$ sites' contents, as inferred from Mössbauer spectroscopy or LCF of their corresponding XANES spectra (b).*

Quantifying the catalysts' average spin state

As briefly discussed above, understanding the relation between these Fe-catalysts' performance and the spin, oxidation and structural state of their Fe-N$_x$ sites is crucial to develop better performing and longer lasting materials. In the specific case of the spin state, its average value for a given catalyst *(S)*

results from the partial contributions of the i components that constitute it, i.e.

$$S = \sum s_i \cdot x_i$$

where s_i and x_i correspond to the individual spin state and relative content of each of those i phases, respectively. As shown above, MS allows estimating the values of x_i in a given catalyst; thus, if a technique allowing the quantification of S would be applied to as many catalysts as components need to be addressed, it should be possible to estimate the individual spin states of these components (s_i).

Luckily, XES is ideally suited for this quantification of the average spin state (S) [11], and was therefore applied to characterize two different Fe-based catalysts pre-characterized through MS and that only featured D1 and D2 doublets assignable to Fe-N$_x$ sites.

On top of these materials, four reference compounds consisting of atomically dispersed Fe-ions coordinated by N-functionalities in a carbon backbone (i.e., structurally resembling the Fe-N$_x$ sites in Figure 1) and with known spin states (from $S = 0$ to 5/2) were also characterized by XES. As displayed in Figure 4a, the recorded spectra consist of a main feature (so-called K$_{\beta1,3}$) and a smaller peak (K$_{\beta'}$) that is not present in the XES of low spin, ferrous compounds (i.e., with $S = 0$); nevertheless, for higher-S compounds, its contribution to the overall spectrum increases with their spin state. Concomitantly, when the areal weight of the K$_{\beta'}$ component in the compounds' X-ray emission spectra is plotted against their known spin state, a linear relation among variables is unveiled (cf. Figure 4b). The subsequent interpolation within this linear trend of the XES-derived K$_{\beta'}$ fraction featured by one of the Fe-based catalysts leads to an estimated S-value of 0.9 for this material.

Having determined these Fe/N/C-catalysts' S-values, their doublets' spin states (s_i) could be quantified providing that their relative composition (x_i) could also be precisely estimated. However, this requires MS-measurements at 4–5 K, since recent studies including MS-tests at such low temperatures have revealed the presence of iron oxide nanoparticles that cannot be discerned in room temperature MS measurements [8]. Therefore, our ongoing efforts focus on the completion of such low temperature MS-measurements, which will ultimately allow a precise and unprecedented quantification of the spin states of these catalysts' Fe-N$_x$ sites.

Conclusions

In summary, this contribution has provided two particular examples of how XAS and XES can help to unveil a material's composition, in this case within the context of Fe/N/C-electrocatalysts. In the first case, the linear combination fit of XANES spectra led to the quantification of the relative content of Fe-N$_x$ sites in these materials, which was consistent with the corresponding MS results. Subsequently, we illustrated the applicability of XES to quantify the average spin state of these catalysts, which in the near future will allow determining the individual spin states of their Fe-N$_x$ sites.
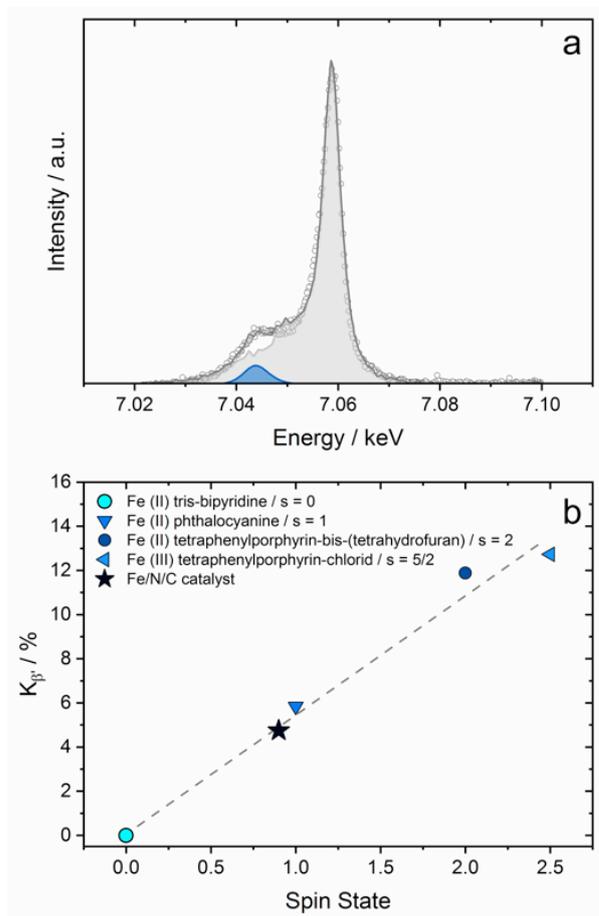
Figure 4. X-ray emission spectrum of an Fe-based catalyst for which MS measurements unveiled the exclusive presence of two doublets assignable to Fe-N$_x$ sites (a). Relation between the spin state and the areal fraction of the K$_{\beta'}$ spectral component of four reference iron compounds, along with the corresponding interpolation along the fitted line for the Fe/N/C catalyst in featured 'a' (b).

Contact

For further information, please contact Dr. Juan Herranz.

juan.herranz@psi.ch

Contributors

The contributors for this particular research topic are K. Ebner, V.A. Saveleva, L. Ni[1], G. Smolentsev[2], T.J. Schmidt, M. Nachtegaal[2], U.I. Kramm[1], J. Herranz.

Acknowledgement

[1] Technische Universität Darmstadt, Darmstadt, Germany
[2] *In situ* X-ray Spectroscopy group, Paul Scherrer Institut

References

[1] J. Herranz, J. Durst, E. Fabbri, A. Pătru, X. Cheng, A.A. Permyakova, T.J. Schmidt, *Nano Energy* **29**, 4–28 (2016).

[2] J. Durst, A. Rudnev, A. Dutta, Y. Fu, J. Herranz, V. Kaliginedi, A. Kuzume, A.A. Permyakova, Y. Paratcha, P. Broekmann, T.J. Schmidt, *Chimia* **69**, 769–776 (2015).

[3] O. Gröger, H.A. Gasteiger, J.-P. Suchsland, *J. Electrochem. Soc.* **162**, A2605–A2622 (2015).

[4] E. Proietti, F. Jaouen, M. Lefèvre, N. Larouche, J. Tian, J. Herranz, J.-P. Dodelet, *Nat. Commun.* **2**, 416 (2011).

[5] W. Ju, A. Bagger, G.-P. Hao, A.S. Varela, I. Sinev, V. Bon, B. Roldan Cuenya, S. Kaskel, J. Rossmeisl, P. Strasser, *Nat. Commun.* **8**, 944 (2017).

[6] U.I. Kramm, J. Herranz, N. Larouche, T.M. Arruda, M. Lefevre, F. Jaouen, P. Bogdanoff, S. Fiechter, I. Abs-Wurmbach, S. Mukerjee, J.-P. Dodelet, *Phys. Chem. Chem. Phys.* **14**, 11673–11688 (2012).

[7] A. Zitolo, V. Goellner, V. Armel, M.-T. Sougrati, T. Mineva, L. Stievano, E. Fonda, F. Jaouen, *Nat. Mater.* **14**, 937–942 (2015).

[8] S. Wagner, H. Auerbach, C.E. Tait, I. Martinaiou, S.C.N. Kumar, C. Kübel, I. Sergeev, H.-C. Wille, J. Behrends, J.A. Wolny, V. Schünemann, U.I. Kramm, *Angew. Chem. Int. Ed.* **58**, 10486–10492 (2019).

[9] T. Mineva, I. Matanovic, P. Atanassov, M.-T. Sougrati, L. Stievano, M. Clémancey, A. Kochem, J.-M. Latour, F. Jaouen, *ACS Catal.* **9**, 9359–9371 (2019).

[10] K. Ebner, J. Herranz, V.A. Saveleva, B.-J. Kim, S. Henning, M. Demicheli, F. Krumeich, M. Nachtegaal, T.J Schmidt, *ACS Appl. Energy Mater.* **2**, 1469–1479 (2019).

Progress towards next-generation negative electrodes for high-energy-density Li-ion batteries

Today, Li-ion rechargeable batteries are the dominant power sources for portable electronics. However, the fast-growing energy-demand of emerging applications, such as electric vehicles and large-scale stationary storage, requires Li-ion batteries with improved specific energy, energy density and power. Despite the fact that the limiting component in Li-ion batteries is, in most cases, the positive electrode, an increase in capacity of the negative electrode can significantly improve the energy density of the entire cell. Today the standard negative electrode in Li-ion battery is graphite, which, however, has reached its limits in terms of performance improvement, as its practical specific charge is almost at its theoretical value. Nevertheless, this specific charge is not sufficient for future batteries, given the growing need for higher energy-density.

Despite the success of the Li-ion batteries, substantial improvements are still necessary in terms of both energy density enhancement and cost reduction, especially to allow for the construction of fully electric vehicles (EV) with >400 km range for the non-luxury, mass automotive market. Therefore, there is a high market-demand for improved battery materials that can be used by Li-ion battery producers without fundamentally changing their battery design and manufacturing processes.

Graphite is a very special material among all Li-ion battery electrode materials due to its high practical capacity of 370 mAh/g, and a low average reduction potential (0.1 V vs. Li$^+$/Li), close to metallic lithium. However, its practical capacity cannot be further improved as it is already near its theoretical limit and other pathways have to be found to improve the performance of the negative electrodes. Even if positive electrode materials are limiting the energy densities of the batteries to a large extent, the increase in negative electrode's capacity results in significantly improved gravimetric and, especially, volumetric energy densities [1], as shown in Figure 1. In comparison with graphite (current situation), silicon–carbon (Si–C) composite as active material, with a designed capacity of 500 mAh/g, results in a significant increase in both volumetric and gravimetric energy densities.

Therefore, use of electrodes containing graphite with capacity enhancing additive, be it an alloying [2] or conversion material [3], is a direct way to enhance the capacity of the negative electrode. Batteries, based on a graphite–Si-alloy blend have so far proven superior to electrodes based purely on Si-nanoparticles [4]. In fact, high theoretical capacity of 3579 mAh/g makes Si an attractive choice as a capacity enhancing additive [2]. Blending Si with the much more stable graphite particles promises a reduction in the stress on the electrode level, which is present in Si electrodes due to the large volume changes during the alloying/de-alloying reactions between Li$^+$ and Si [5]. In addition, a large fraction of a conductive component, such as graphite, can also mitigate electronic contact losses in case of volume changes [6]. The capacity-enhancing additive can be not only Si but as well other elements and compounds possessing high capacity and low potentials vs. Li$^+$/Li, such as Sn, SnO$_2$, P, Sb, etc.

The further enhancements can be achieved by fully replacing graphite by one of capacity enhancing additives, and here possible solutions are even more challenging, as mentioned above, however, with much larger energy density increase due to much higher capacity to uptake Li-ions.

Within the Electrochemistry Laboratory, we pursue improvements within all negative electrode variants, as each of them have their niche and specific applications. Different requirements on energy density, weight, volume and safety (and combinations of them) are needed in different industry sectors.
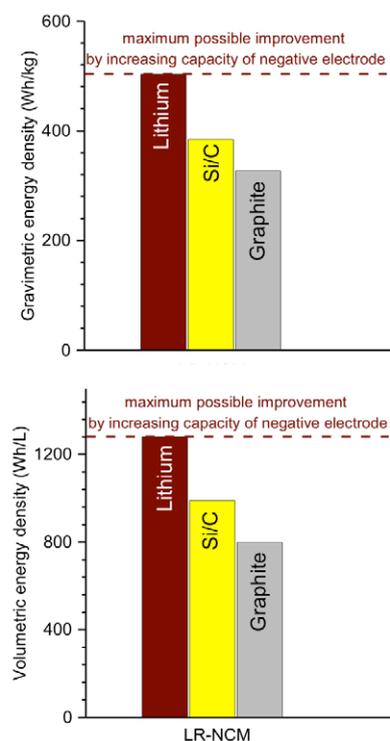
Figure 1. Gravimetric and volumetric energy density dependence on capacity of anode. Si–C composite contains 8 % of Si, resulting in a composite capacity of 500 mAh/g. Each negative electrode is paired with LR-NCM (lithium-rich nickel-cobalt-manganese oxide) positive electrode for energy density calculations.

Silicon as capacity-enhancing additive

Estimations of the energy density in dependence of the Si content in the negative electrode suggest that a Si content of less than 50 wt.% is sufficient to maximize the energy density of a graphite [7]. However, such estimation does not account for energy efficiency: when comparing the voltage profiles of graphite, silicon and graphite–Si half-cells, it is evident that the

area between the lithiation and delithiation branches increases considerably with increase of the Si content, meaning that the round-trip efficiency of the electrode reduces.

The electrode capacity fading (Figure 2) seems to proceed in three stages. Initially, the discharge capacities are close to the theoretically expected values but within the first 50 cycles the slopes of the capacity fade are steeper than for the following cycles. This initial stage is seen most clearly for electrodes containing 15 wt.% and 20 wt.% Si, but is also present in electrode formulations with less Si.
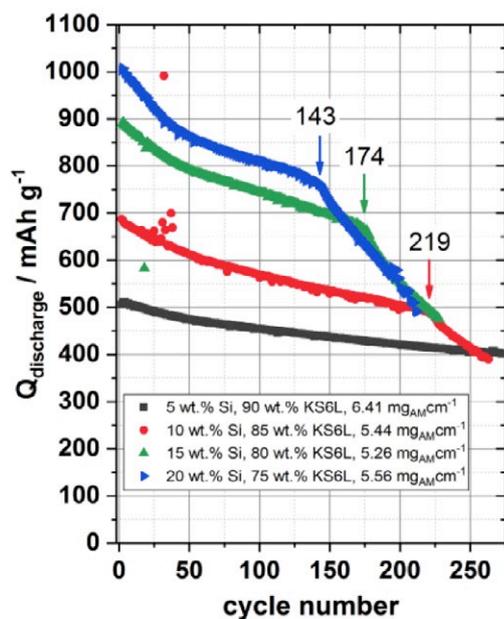
Figure 2. Cycle life in dependence of silicon content in graphite–silicon half-cells. The onset of electrode breakdown is indicated by an arrow and the cycle number. Electrolyte: LP30 + 4 wt.% FEC.

The capacity fading slows down in the second stage, where the capacity loss per cycle is approximately constant in this region and is, again, more pronounced in electrodes with higher Si contents. The third stage is marked by a distinct drop in discharge capacity, and indicates the end of the cycle-life of the electrode. The electrode performance breakdown correlates directly with the Si content, but not in a linear fashion. The cycle life of graphite–Si electrodes depends on the concentration of the electrolyte additive fluoroethylene carbonate (FEC) and its rate of consumption at the electrode surface. This makes the observed trends in capacity retention (Figure 2) not only dependent on Si content (and electrode area), but also on mass loading and the absolute amount of FEC in the cell, highlighting the importance of similar mass loadings and electrolyte volumes for comparison studies. Moreover, electrodes with higher capacities (i.e., more Si) degrade the Li counter electrode faster, because more Li is stripped and plated during cycling. Thereby the electrodes promote the growth of Li dendrites and the formation of mossy Li. In previous work by our group it was also shown that the local dendrite growth is facilitated by the large difference in capacity between graphite and silicon [8].

The performance of graphite electrodes with Si as capacity-enhancing additive are strongly dependent on electrode morphology and homogeneity, therefore, cross-sections of graphite electrodes with different Si contents were imaged by scanning electron microscopy (SEM) as shown in Figure 3.
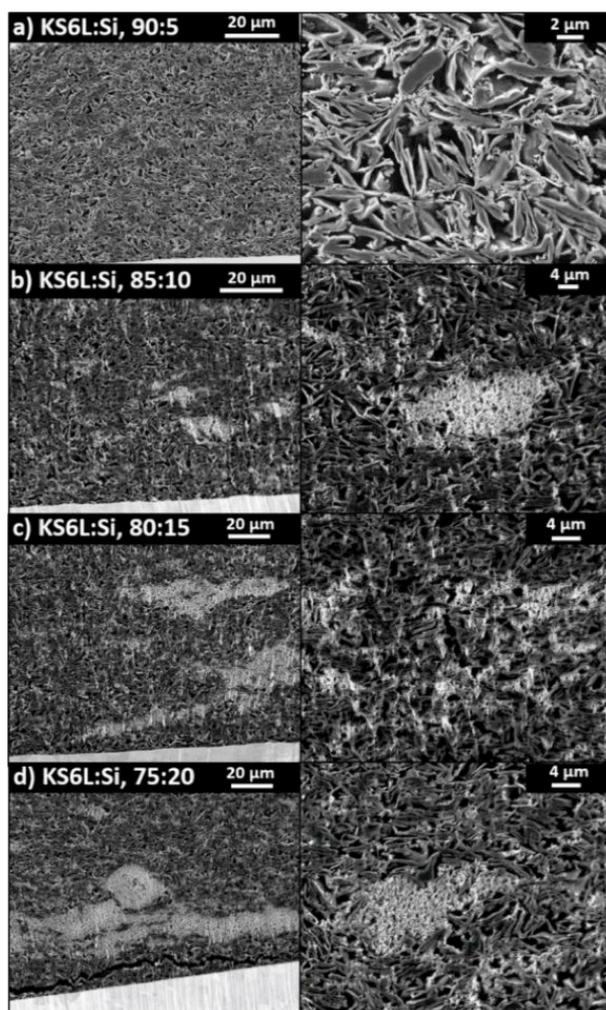
Figure 3. SEM micrographs of cross-sections of pristine KS6L–Si electrodes with Si contents of 5, 10, 15 and 20 wt.%. On the right: images at higher magnification.

With the exception of the electrode containing 5 wt.% of Si, the electrodes have large agglomerates of Si. The Si particles in the 5 wt.% Si sample are located mostly between the graphite particles or form smaller agglomerated domains (<2 μm) in the void space. Already with 10 wt.% Si, some agglomerated Si domains with sizes >10 μm can be found in the electrode. As Si agglomeration and the inhomogeneity of the electrode increases, the Si domains are likely to induce additional stress in the KS6L–Si electrodes and can cause the disintegration and electronic disconnection of subdomains. The domain disconnection could explain the initial capacity drop over the first 50 cycles as shown in Figure 2, assuming that agglomerated Si domains disconnect faster than the fraction of well-dispersed Si in the rest of the electrode.

Si-particle agglomeration can be addressed by various methods, while we pursued investigation of the impact of different types of graphites on the electrochemical performance of graphite–Si electrodes. Further, the KS6L graphite is representative for materials with small particle sizes (average size = 3.5 μm), while SFG44 and Actilion 1 feature much larger particle sizes: 24 and 13 μm, respectively. The large-particle-size graphites also have different shape of the particles, where SFG44 has platelet-like and Actilion 1 more rounded particles, see Figure 4 (right).
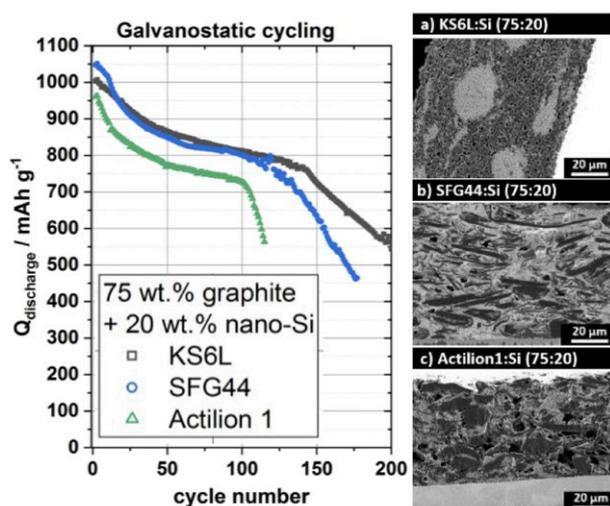
Figure 4. *Discharge capacities of graphite-silicon electrodes comprised of 75 wt.% graphite and 20 wt.% nano-Si (30–50 nm) and inactive ingredients, such as binder and conductive additive. SEM cross-section images of graphite–Si electrodes (w/w = 75:20), containing a) KS6L, b) SFG44 and c) Actilion 1.*

One can also see that Si addition into the blend with largest graphite particles (SFG44) leads to inverse morphology – it seems that graphite particles are embedded into the matrix of Si (Figure 4) with large void space. Nevertheless, the performance of this electrode is as good as of the electrode containing small-particle-sized graphite KS6L. On the other hand, the electrode with SFG44 looks much more homogeneous than with KS6L, only less dense. In case of Actilion 1 graphite, exhibiting the lowest capacity and the most extensive capacity fading of all three studied graphites (Figure 4), the electrode had high void density and poor contact, explaining the poor performance.

Tin oxide as capacity-enhancing additive

The combination of SnO_2 and graphite in a composite electrode allows to obtain a Li-ion battery negative electrode with enhanced specific charge. However, the reported cycling stability of these electrodes is often rather poor. The conditions under which long-term cycling for these electrodes can be achieved, determined by studying the effects of the electrode and electrolyte composition, as well as of the cycling protocol on the cycling stability of SnO_2–graphite electrodes, have been established.

Firstly, it has been observed that capacity fading is delayed if upper potential cut-off does not exceed 1 V [9], as up to 1 V the mechanism is mainly based on alloying reaction, while above that full conversion is happening upon lithiation. Potential cut-off at 1 V limits the achieved capacity (500 mAh/g) as compared to cycling up to 1.2 V (540 mAh/g), but this loss is not very high if capacity retention is improved (Figure 5a).

Gaining stable long-term cycling, especially for negative electrode materials, is often achieved by using electrolyte additives; one of the most favorable is FEC. Addition of only 2 wt.% of FEC to the standard LP30 electrolyte (1 M $LiPF_6$ in EC:DMC (1:1)) led to improved capacity retention by 30 % (Figure 5b). However, FEC is a sacrificial additive and it is expected that, when it is consumed, the insulating layer due to EC decomposition will appear.
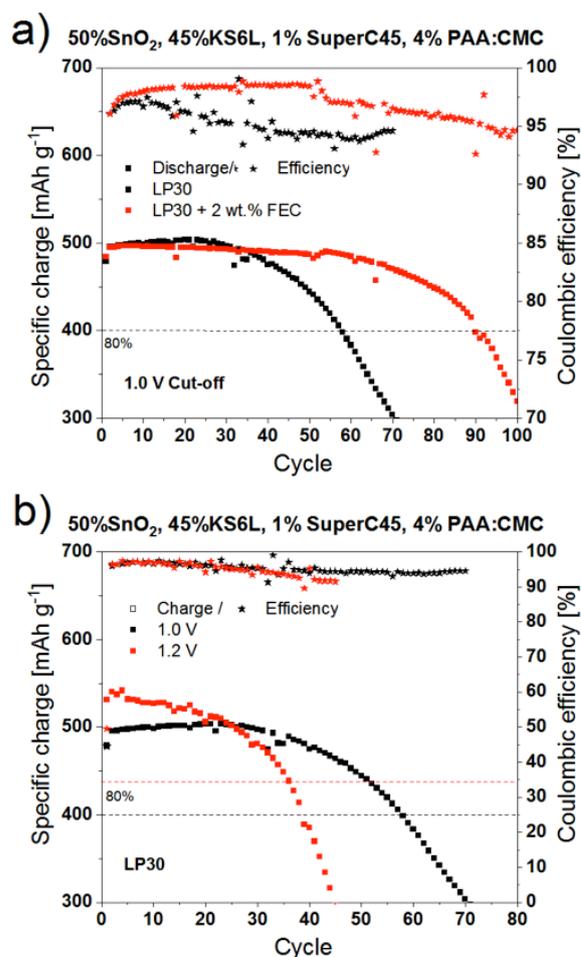
Figure 5. *a) Electrochemical performance of 50 % SnO_2–45 % KS6L electrodes cycled with LP30 electrolyte using 1.0 V (black) and 1.2 V (red) delithiation cut-off potential. b) Electrochemical performance of 50 % SnO_2–45 % KS6L cycled with LP30 (black) and LP30 + 2 wt.% FEC (red), and electrochemical performance of KS6L graphite electrodes.*

Therefore, a post-mortem SEM study was carried out on electrodes cycled with and without FEC additive, to identify reasons for the specific-charge fading (Figures 5b and 6).
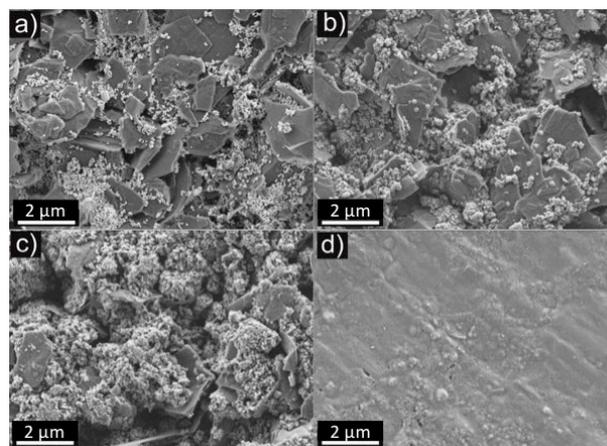
Figure 6. *Micrographs of 50 % SnO_2–45 % KS6L electrode cycled with LP30 + 2 wt.% FEC electrolyte. a) pristine, b) after 25 cycles, c) after 75 cycles, d) after 150 cycles.*

Electrodes were analyzed after 25, 75 and 150 cycles. These specific cycles were chosen to evaluate the electrode mor-

phology in the presence of FEC (25 cycles), after FEC is fully consumed (75 cycles) and after the battery specific charge reaches zero (150 cycles) (Figure 5b). From the SEM analysis, we could see that the hypothesis was correct and after 75 cycles we start to see electrode's surfaces changes, while after 150 cycles electrode itself is not visible anymore as it is covered by electrolyte decomposition products.

Building upon this result, addition of larger fractions of FEC in the electrolyte have been studied to find out if cycle-life can be extended by adding optimal amount of sacrificial additive FEC. As can be seen in Figure 7, the increase of FEC fraction has extended the time until electrodes reach 80 % of capacity retention significantly, and 300 cycles could be successfully reached. Moreover, it seems that EC component is needed for long-term performance, because, as can be seen in Figure 7, after about 200 cycles, the cell in electrolyte without EC starts to lose more capacity than the one with EC present.
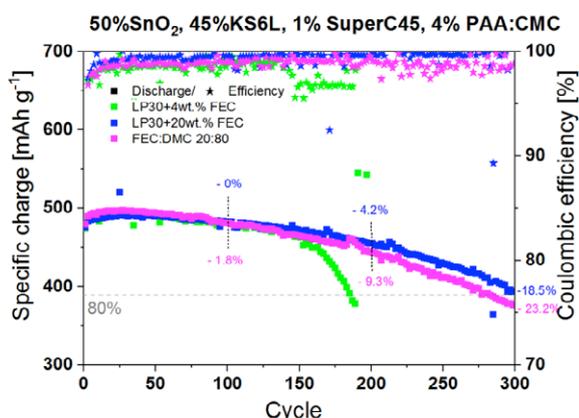
Figure 7. *Electrochemical performance of 50 % SnO$_2$–45 % KS6L cycled in LP30 with 4 wt.% and 20 wt.% FEC; as well as electrolyte with solvent composition FEC:DMC 20:80, where EC is replaced by FEC. The percentages indicate the specific charge loss after 100, 200 and 300 cycles.*

The amount and type of binder, in combination with an optimized amount of electrolyte additive and applied limitation to the delithiation cut-off potential, play a major role in stabilizing performance of these electrodes. A specific charge retention of 81.5 % after 300 cycles was obtained for electrodes prepared with 50 wt.% SnO$_2$, KS6L graphite, PAA:CMC binder, cycled with FEC electrolyte additive using 1.0 V delithiation cut-off potential as final optimal conditions for graphite electrodes with tin oxide as capacity-enhancing additive [9].

Conclusion

Li-ion battery negative electrode performance can go far beyond the graphite, which is dominating the current market. In this report we have shown two alternative negative electrodes, where the capacity of electrode and energy density of cell can be increased by adding small amounts of capacity-enhancing electrode additives. The further gains can arise by fully replacing graphite by one of capacity-enhancing additives, and here possible solutions are even more challenging, however, with much larger energy-density increase due to much higher capacity of the active material.

However, as can be seen in Figure 1, the most significant improvement, and as well the largest theoretically possible, would be reached by replacing the lithium-matrix materials by metallic lithium itself. In this case, the change of terminology would be also required, as we start to talk about lithium-metal batteries and not lithium-ion batteries anymore. Enabling metallic lithium negative electrodes is mainly motivated by significant increase of energy density in regards to both weight and volume, despite the excess of metallic lithium needed to ensure stable potential and cycling. In post-lithium-ion batteries, the gain is twice as compared to graphite, while for current Li-ion battery positive electrodes it is about 30 %. Metallic lithium as negative electrodes has been under investigation since early 70-ies of the last century and declined with the invention of Li-ion battery technology, as it was considered a safer alternative. However, recently interest in the metallic lithium as negative electrode has spiked again due to expected high future gains as well as development of analytical tools, enabling to revisit metallic lithium topic to fully understand underlying failure mechanism and, hopefully, to offer viable solutions.

Contact

For further information, please contact Dr. Sigita Trabesinger, head of Battery Electrodes and Cells Group.

sigita.trabesinger@psi.ch

Contributors

The contributors for this particular research topic are Dr. Fabian Jeschull, Dr. Yuri Surace, Dr. Tiphaine Schott.

Acknowledgement

References

[1] E.J. Berg, C. Villevieille, D. Streich, S. Trabesinger, P. Novák, *J. Electrochem. Soc* **162**, A2468–A2475 (2015).

[2] M.N. Obrovac, V.L. Chevrier, *Chem. Rev.* **114**, 11444–11502 (2014).

[3] A. Trifonova, M. Winter, J.O. Besenhard, *J. Power Sources* **174**, 800–804 (2007).

[4] M. Marinaro, D.-H. Yoon, G. Gabrielli, P. Stegmaier, E. Figgemeier, P.C. Spurk, D. Nelis, G. Schmidt, J. Chauveau, P. Axmann, M. Wohlfahrt-Mehrens, *J. Power Sources* **357**, 188–197 (2017).

[5] H. Chen, Z. Wang, X. Hou, L. Fu, S. Wang, X. Hu, H. Qin, Y. Wu, Q. Ru, X. Liu, S. Hu, *Electrochim. Acta* **249**, 113–121 (2017).

[6] D. Mazouzi, Z. Karkar, C. Reale Hernandez, P. Jimenez Manero, D. Guyomard, L. Roué, B. Lestriez, *J. Power Sources* **280**, 533–549 (2015).

[7] F. Jeschull, Y. Surace, S. Zürcher, M.E. Spahr, P. Novák, S. Trabesinger, *Electrochim. Acta* **320**, 134602 (2019).

[8] T. Schott, J.L. Gómez-Cámer, C. Bünzli, P. Novák, S. Trabesinger, *J. Power Sources* **343**, 142–147 (2017).

[9] Y. Surace, F. Jeschull, T. Schott, S. Zürcher, M.E. Spahr, S. Trabesinger, *ACS Appl. Energy Mater.* **2**, 7364–7374 (2019).

The SCCER «Heat and Electricity Storage» – Highlights 2019

The Swiss energy system is facing substantial transformation and associated challenges: While nuclear power plants will be gradually phased out, power generation from photovoltaics and wind is supposed to (partially) fill the resulting gap. At the same time, the energy system is expected to reduce its carbon-dioxide (CO_2) emissions in order to meet climate goals in line with the Paris Agreement. An electricity system largely based on intermittent renewables needs temporal flexibility options buffering generation and demand. One of those flexibility options is «Power-to-X» (P2X): This term describes the electrochemical conversion of electricity into gaseous or liquid energy carriers or industrial feedstocks.

Access to energy is a key pillar of our society. The energy growth of the past decades was primarily backed by an increasing consumption of fossil fuels and nuclear energy. Today, it looks like we run out of climate before we run out of fossil fuels. Cleaner, safer and more economic ways of powering the society are in implementation worldwide. While the options of renewable energy differ across geographies, for places in central Europe without access to coastlines, sun, on-shore wind and hydropower are the major future power sources.

Situation for Switzerland

For Switzerland mainly hydropower, sun, and, due to topography and acceptance challenges, wind in limited capacity, represent a significant potential for future power generation. The seasonal production profile of sun and wind distinguishes from, for instance, existing band energy from nuclear, as it provides limited coverage of demand in fall and spring. This

results in an energy shortage requirement of some weeks in late fall and early spring, depending on the allowable wind capacity and import acceptance. [1]

In Switzerland, long term energy storage in significant amounts are required to mitigate such shortage. From today's perspective, only chemically stored energy is able to fulfil this requirement, as the usable storage capacity of pump storage plants is limited and battery systems lead to high storage costs if operated for seasonal storage. For this purpose, and to reduce greenhouse gas (GHG) emissions of the demand sectors of the energy system (e.g. aviation) synthetic production of fuels from renewable energy is an option.

The white paper «Perspectives of Power-to-X technologies in Switzerland» [2], is a joint effort of the SCCERs *Heat and Electricity Storage, Biosweet, Mobility, Crest* and *Furies,* with the aim to derive a technical, economic, environmental, systemic and regulatory assessment of Power-to-X (P2X). It describes

Power System Perspective
- Present and future situation
- Grid stability
- Ancillary services
- Requirements for sizing and siting of P2X in electrical grids
- Techno-economic analysis with focus on market integration

Techno-Economic Perspective
- P2X pathways
- Key components and processes
- Costs and technical performance

CO_2 Sources and Markets
- Biogenic
- Industrial
- Direct Air capture

H_2

CO_2

CH_4

Regulatory & Policy Perspective
- Law affecting all P2X systems
- Law affecting P2X in the markets
  - Electricity
  - Transport
  - Heating
- Innovation policy

Environmental Perspective
- Life Cycle Analysis
- Compare P2X with conventional technology

End-use Market Analysis
- Gaseous fuels CH_4, H_2
- Transport sector
- Industry sector H_2, CH_4 as feedstock
- Combined revenues

Figure 1. Schematic representation of the scope of the White Paper.

the state of the art knowledge concerning electrochemical conversion but does not address electro-thermal conversion (Figure 1).

In the following some findings, taken from the comprehensive report accompanying the white paper [3], are presented. Three characteristics of Power-to-X are relevant for Switzerland:
- It provides the required flexibility to a future energy system largely based on renewables.
- It provides a fuel which can be stored long term and can be used in transportation and heat sector to replace fossil fuels.
- It enables Switzerland to reach the self-set greenhouse gas reduction target cost-effectively.

While the mentioned qualities of Power-to-X processes are widely accepted, for the economic aspects no common understanding exists. Electricity companies are exploring the field by erecting pilot plants, dealing with ill-defined regulations and the lack of standards. Based on existing literature, the white paper attempts to quantify the economics in dependence on the different markets, the environmental benefits, as well as the influence of regulation and the legal framework.

Electricity demand aspects

The white paper considers hydrogen, methane, liquid fuels for end-use purposes and for re-electrification in detail (Figure 2), while this article exemplarily focuses on the aspects of methane. Ammonia and heat are also valuable products but not discussed in depth. All processes discussed here start with the production of hydrogen from renewable electricity. Electrolyzers are a key component in Power-to-X plants for which a range of electrolyser technologies (alkaline, PEM, SOEC) is considered and the specific hydrogen production costs are compared. Since for electrolyzers the investment costs are significant, the two factors dominating the economics of Power-to-X are the annual operating hours (determining annualized investment costs) and the price for electricity. At about 50 % annual utilization (4500 hrs) the electricity costs dominate the economics. This has implications for the concept of electricity generation used for Power-to-X processes on one hand and for the political aspects of electricity pricing (specifically network charging). [2]

If large capacity of PV or wind is installed, P2X becomes most valuable for balancing the lowest grid level, which is due to its current layout most vulnerable for imbalances. The magnitude of installable PV is a political sensitive topic, but based on pure geographic (supply side) and physical consideration (demand side) about 25 TWh/a, currently supplied by the installed 3.3 GW (25 TWh/a) capacity of nuclear power, need to be replaced. Here any compensation of losses due to seasonal storage is excluded. On the supply side, various assumptions have to be made (like for PV efficiency of the cells, installation on vertical surfaces…) and the potential for e.g. PV ranges from 15 TWh up to 50 TWh. If wind is allowed, even the most conservative PV scenario shows that the required power to replace the nuclear capacity is possible, but requires seasonal balancing strategies. It is estimated that the required 25 TWh of PV sourced energy has a seasonal production split of 63 % in summer and 37 % in winter. This results roughly in 13 % of the annual production in PV to be shifted seasonally (3.25 TWh net). Based on the 25 TWh estimation and considered overall storage losses (50 %), about 32 TWh of new renewable electricity
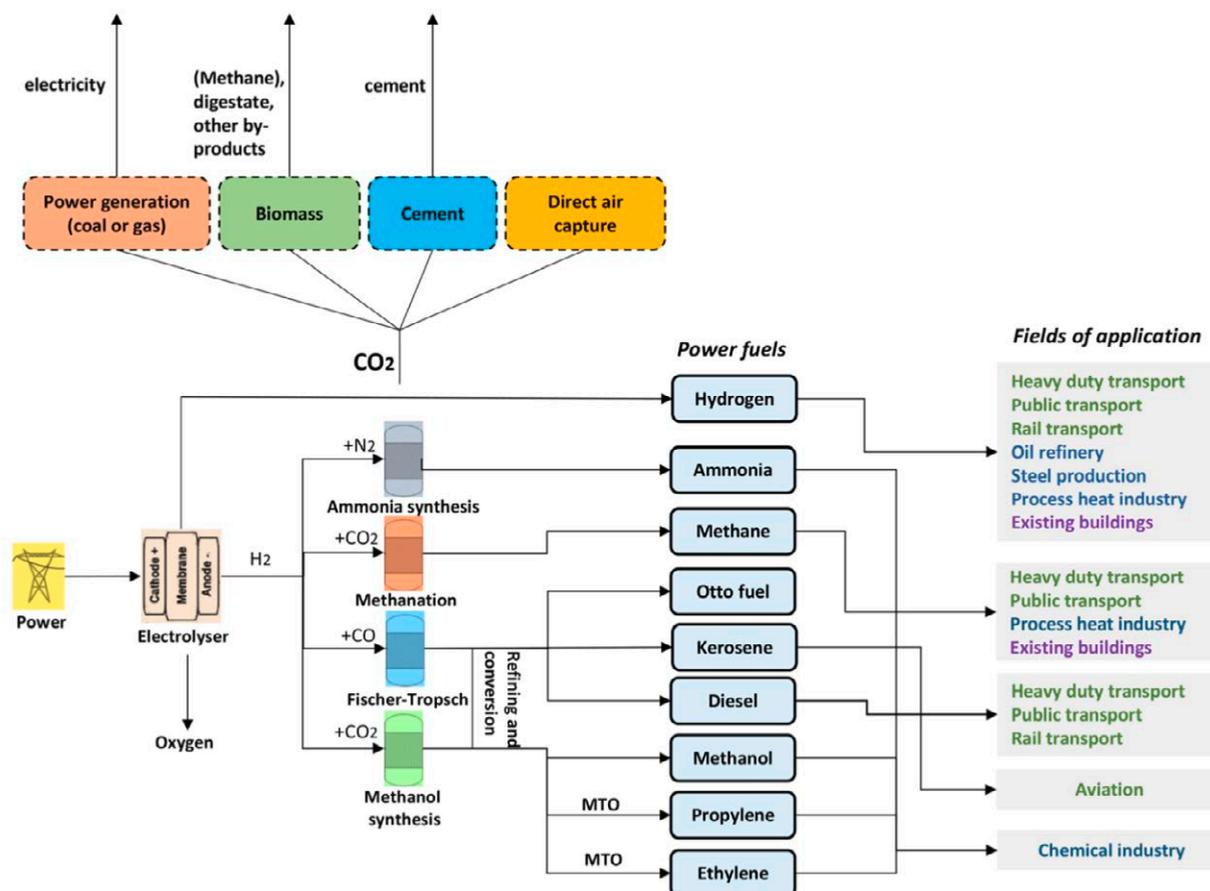
Figure 2. *System scheme of different P2X production chains with technology alternatives (based on [8]).*

is required while 7 TWh have to be provided for the seasonal shift. Power-to-X technology is one of the available options to manage the seasonal flexibility. This consideration excludes wind, which is discussed controversially, but has a better production characteristic in winter time, mitigating the storage challenges. [3]

The economics is not only driven by the capital costs, but also by the operating costs, mainly the electricity. Any price component added to the price for electricity (grid fee, taxes…) challenges the business case for Power-to-X plants. The players in the field demand an exemption from grid fee for the electricity stored in power to gas if done in a system stabilizing fashion (according to the regulation for pump storage) for this very reason. [4]

Ressource aspects

Besides of the cost for P2X a key question is the source of CO_2 for X for the production of hydrocarbons like CH_4 or liquid synthetic fuels. For power to hydrocarbons being part of the solution and not part of the problem, the CO_2 has to come out of the atmosphere (source 1), from a biogenic source (source 2) or as a dual use of CO_2 from a non-renewable source like calcination of limestone for cement industry, waste incineration (plastic, bio waste) or large centralized power generation (source 3) as they are larger point source CO_2 emitters.

The latter two are considered as «waste streams», so there is no, or even a negative price associated with the raw CO_2. Depending on the technology, the raw CO_2 from sources 2 and 3 needs to be purified, creating additional costs. CO_2 pricing is therefore an enabler for all three sources creating additional revenues, compensating for the cost of treatment of raw CO_2, since the costs for emitting CO_2 are transferred to the final emitter. While CO_2 taken out of the air is unlimited in supply, but at significant cost (today: 600 CHF/ton), the sources 2 and 3 are comparably less expensive but limited in supply. Studies estimate the max. potential from the larger point sources to 7 314 000 T/a resulting in a storage capacity of about 39 TWh/a (as methane). If the society becomes CO_2 neutral or even CO_2 negative in the long run, all fossil sources (waste) and cement plants are no longer available. Today the waste, converted in waste incineration plants contains about 50 % non-renewable waste [5] which limits the CO_2 from waste incineration plants significantly. Assuming a reduction of waste-born CO_2 by 50 %, and excluding the cement plants (since this is non-renewable CO_2 which has to be taken out of the loop), the methane storage potential drops from 39 TWh/a (7 314 000 T/a CO_2) to 13 TWh/a (2 482 000 T/a CO_2). Based on this estimation, a conversion efficiency of 27 % from methane to power can be allowed without taking CO_2 from air directly in order to store required 3.5 TWh for the seasonal shift. The storage capacity for methane of Switzerland (incl. the storage in Etrez, France) is little more than 1.6 TWh. In order to store the seasonal energy in the form of methane eight-times this capacity is needed without consideration of seasonally shifted net-imports. [6]

Power to hydrocarbon not only is an option for long term storage as described above, but also provides plug-in fuels for today's long distance transportation and the heating sec-

tor. Today's gas market has a volume of 39 TWh, with highest demand between October and April. [7] Based on today's CO_2 capacity this could be just matched, but then nothing is left for the electricity and the transportation sector. For the mid-term power to methane is an option, but in the long run, cheap CO_2 air capture or a carbon free energy carrier like hydrogen are needed.

Conclusion

Concluding the considerations, it is obvious that the transition from today's fossil based economy with nuclear power to a de-fossilized economy without nuclear power is possible. But it is also obvious that a careful and holistic management of the transition is required since the resources in terms of energy and feedstock are limited, not allowing for a pre-disclosure of options like wind energy or storage option. The perspectives of power to gas from a systemic view are given. From the economic view, the electricity price, the cost for hydrogen production and the cost of CO_2 emission versus the cost of CO_2 air capture are the most relevant parameters.

Contact

For further information on the SCCER Heat and Electricity Storage please contact Dr. Jörg Roth.

joerg.roth@psi.ch

References

[1] F. Huneke, C. Perez Linkenheil, M. Niggemeier, KALTE DUN-KELFLAUTE, Greenpeace Energy eG, 2017.

[2] T. Kober, C. Bauer (eds.), C. Bach, M. Beuse, G. Georges, M. Held, S. Heselhaus, P. Korba, L. Küng, A. Malhotra, S. Moebus, D. Parra, J. Roth, M. Rüdisüli, T. Schildhauer, T.J. Schmidt, T.S. Schmidt, M. Schreiber, F.R. Segundo Sevilla, B. Steffen, S.L. Teske, *White Paper «Power-to-X: Perspectives in Switzerland»* (2019). (White Paper of the corresponding Joint Activity of the Swiss Competence Centers for Energy Research, www.sccer-hae.ch; DOI 10.3929/ethz-b-000352294.)

[3] P. Korba, R. Segundo, S. Teske, M. Rüdisüli, *3.2 Aspects for P2X technology integration into the power system*. In T. Kober, C. Bauer (eds.), *White Paper «Power-to-X: Perspectives in Switzerland»*, 31–40 (2019).

[4] M. Schreiber, S. Heselhaus, *4.2 View o P2X from the legal perspective – the regulatory framework*. In T. Kober, C. Bauer (eds.), *White Paper «Power-to-X: Perspectives in Switzerland»*, 77–83 (2019).

[5] U Steiger, *Erhebung der Kehrichtzusammensetzung 2012*, Bundesamt für Umwelt BAFU (2014).

[6] T.J. Schildhauer, *3.1 Sources of carbon/CO2 for synthetic hydrocarbon production*. In T. Kober, C. Bauer (eds.), *White Paper «Power-to-X: Perspectives in Switzerland»*, 23–30 (2019).

[7] S. Moebus, *3.3 P2X as potential newcomer in markets for gaseous fuels*. In T. Kober, C. Bauer (eds.), *White Paper «Power-to-X: Perspectives in Switzerland»*, 41–47 (2019).

[8] Deutsche Energie-Agentur, *Power to X: Technologien*. Berlin: Strategieplattform Power to Gas (2018).

THE ELECTROCHEMISTRY LABORATORY

FACTS & FIGURES

STRUCTURE 2019

Electrochemistry Laboratory (LEC)

Laboratory Head
Dr. F.N. Büchi a.i.

Assistant
C. Gloor

Staff
Prof. Dr. P. Novák

Battery Materials and Diagnostics

Dr. M. El Kazzi

Battery Electrodes and Cells

Dr. S. Trabesinger

Membranes and Electrochemical Cells

PD Dr. L. Gubler

Fuel Cell Systems and Diagnostics

Dr. F.N. Büchi i.P.

Electrocatalysis and Interfaces

Prof. Dr. T.J. Schmidt i.P.

Neutron Radiography of Electrochemical Systems

Dr. P. Boillat

PERSONNEL 2019

Staff

Dr. Daniel ABBOTT (Post Doctoral Researcher)
Martin AMMANN (Technician)
Dr. Pierre BOILLAT (Group Leader)
Dr. Christoph BOLLI (Post Doctoral Researcher)
Dr. Anthony BOUCLY (Post Doctoral Researcher)
Dr. Felix BÜCHI (Laboratory Head a.i. & Group Leader)
Dr. Magali COCHET (Scientist)
Dr. Salvatore DE ANGELIS (Post Doctoral Researcher)
Emanuele DI GIOVANNI (Engineer)
Dr. Mario EL KAZZI (Group Leader)
Dr. Jens ELLER (Scientist)
Dr. Emiliana FABBRI (Scientist)
Lucy FISCHER (Technician)
Davide GAMPER (Technician)
Cordelia GLOOR (Assistant)
Thomas GLOOR (Technician)
PD Dr. Lorenz GUBLER (Group Leader)
Dr. Fabian JESCHULL (Post Doctoral Researcher)
Dr. Lukasz KONDRACKI (Post Doctoral Researcher)
Dr. Steven LACEY (Post Doctoral Researcher)
Dr. Elena MARELLI (Post Doctoral Researcher)
Dr. Cyril MARINO (Scientist)
Christian MARMY (Technician)
Dr. David MCNULTY (Post Doctoral Researcher)
Dr. Alexander MUROYAMA (Post Doctoral Researcher)
Dr. Tom NOLTE (Post Doctoral Researcher)
Prof. Dr. Petr NOVÁK (Staff)
Dr. Fabio OLDENBURG (PSI Founder fellow / CTO Gaia Membranes)
Dr. Alexandra PĂTRU (Scientist)
Dr. Daniele PEREGO (Post Doctoral Researcher)
Christian PETER (Engineer)
Dr. Quang Hieu PHAM (Post Doctoral Researcher)
Elian PUSCEDDU (PSI Founder fellow / CEO Gaia Membranes)
Dr. Mayank SABHARWAL (Post Doctoral Researcher)
Dr. Viktoriia SAVELEVA (Post Doctoral Researcher)
Dirk SCHEUBLE (Engineer)
Prof. Dr. Thomas J. SCHMIDT (Division Head/Group Leader)
Aaron SCHNEIDER (Lab Technician)
Dr. Aleš ŠTEFANČIČ (Post Doctoral Researcher)
Dr. Sigita TRABESINGER-URBONAITE (Group Leader)
Stephan TSCHUMI (Engineer)
Dr. Claire VILLEVIEILLE (Group Leader)
Dr. David VONLANTHEN (Scientist)
Dr. Leiting ZHANG (Post Doctoral Researcher)

PhD Students

Dino AEGERTER
Kinanti Hantiyana ALIYAH
Ugljesa BABIC
Casey BEALL
Eric Ricardo CARREÓN RUIZ
Piyush CHAUHAN
Jingfeng CHEN
Yen-Chun CHEN
Christoph CSOKLICH
Tym DE WILD
Justus DIERCKS
Nataša DIKLIĆ
Kathrin EBNER
Meriem FIKRY
Eibar Joel FLORES CEDEÑO
Steffen GARBE
Jonathan HALTER
Adrian HEINRITZ
Laura HÖLTSCHI
Baejung KIM
Paul KITZ
Daniela LEANZA
Wenmei LIU
Maria Victoria MANZI OREZZOLI
Marta MIROLO
Adrian MULARCZYK
Mauro POVIA
Bernhard PRIBYL-KRANEWITTER
Simon SCHNEIDER
Tobias SCHULER
Arnaud SCHULLER
Maximilian SCHUSTER
Muriel SIEGWART
Michael STRIEDNIG
Seçil ÜNSAL
Eric WINTER
Xiaohan WU
Hong XU
Mateusz ZLOBINSKI

Members of the Electrochemistry Laboratory in 2019.

DISSERTATIONS 2019

Daniela Leanza

New perception of electrode-electrolyte interfaces in Li-ion batteries enabled by XPEEM spectromicroscopy

Ph.D. Thesis No. 25757, ETH Zürich, January 2019.

Examiners: Prof. Dr. Petr Novák, PSI Villigen/ETH Zürich
Prof. Dr. Jeroen van Bokhoven, PSI Villigen/
ETH Zürich
Dr. Mario El Kazzi, PSI Villigen

Baejung Kim

Perovskites as Electrocatalysts for Oxygen Evolution Reaction for Alkaline Water Electrolysis

Ph.D. Thesis No. 25959, ETH Zürich, April 2019.

Examiners: Prof. Dr. T.J. Schmidt, PSI Villigen/ETH Zürich
Prof. Dr. Christophe Copéret, ETH Zürich

Xiaohan Wu

Operando characterization of degradation phenomena in all-solid-state batteries with a sulfide-based solid electrolyte

Ph.D. Thesis No. 25999, ETH Zürich, May 2019.

Examiners: Prof. Dr. Petr Novák, PSI Villigen/ETH Zürich
Prof. Dr. Markus Niederberger, ETH Zürich
Dr. Mario El-Kazzi, PSI Villigen

Eibar Flores

Development of operando diagnostics for Li-ion cathodes by Raman spectroscopy

Ph.D. Thesis No. 26045, ETH Zürich, June 2019.

Examiners: Prof. Dr. Petr Novák, PSI Villigen/ETH Zürich
Prof. Dr. Renato Zenobi, ETH Zürich
Prof. Dr. Erik J. Berg, PSI Villigen/Uppsala
University

Fabio Oldenburg

Membrane design towards improved vanadium redox flow batteries

Ph.D. Thesis No. 26101, ETH Zürich, June 2019.

Examiners: Prof. Dr. T.J. Schmidt, PSI Villigen/ETH Zürich
Prof. Dr. W. Caseri, ETH Zürich
PD Dr. L. Gubler, PSI Villigen

Ugljesa Babic

Polymer electrolyte water electrolysis: Development of diagnostics methods and mitigation strategies to tackle component degradation

Ph.D. Thesis No. 26105, ETH Zürich, June 2019.

Examiners: Prof. Dr. T.J. Schmidt, PSI Villigen/ETH Zürich
Prof. Dr. D. Poulikakos, ETH Zürich
PD Dr. L. Gubler, PSI Villigen

Mauro Povia

Realization and Application of Operando and Combined A-SAXS and XAS Apparatus for the Study of Pt/C and IrO_2 Catalysts

Ph.D. Thesis No. 26143, ETH Zürich, June 2019.

Examiners: Prof. Dr. T.J. Schmidt, PSI Villigen/ETH Zürich
Dr. J. Herranz, PSI Villigen/ETH Zürich
Prof. Dr. C. Copéret, ETH Zürich

Jonathan Halter

Understanding and Mitigating Phosphoric Acid Migration in High Temperature Polymer Electrolyte Fuel Cells

Ph.D. Thesis No. 26182, ETH Zürich, July 2019.

Examiners: Prof. Dr. T.J. Schmidt, PSI Villigen/ETH Zürich
Prof. Dr. M. Stampanoni, PSI Villigen/ETH Zürich
Dr. F.N. Büchi, PSI Villigen

Paul Kitz

A new Perspective on Interphase Formation in Li-ion Batteries by Combined EIS & EQCM-D

Ph.D. Thesis No. 26169, ETH Zürich, July 2019.

Examiners: Prof. Dr. Petr Novák, PSI Villigen/ETH Zürich
Prof. Dr. Nicholas Spencer, ETH Zürich
Prof. Dr. Erik J. Berg, PSI Villigen/Uppsala University

Muriel Siegwart

Beyond Conventional Neutron Transmission Radiography: Fuel Cell Studies with Time-of-Flight and Dark-Field Imaging

Ph.D. Thesis No. 26343, ETH Zürich, September 2019.

Examiners: Prof. Dr. T.J. Schmidt, PSI Villigen/ETH Zürich
Prof. Dr. T. Lippert, PSI Villigen/ETH Zürich
Dr. P. Boillat, PSI Villigen

Victoria Manzi Orezzoli

Advanced Design of Gas Diffusion Media for High Power Density Polymer Electrolyte Fuel Cells

Ph.D. Thesis No. 26404, ETH Zürich, October 2019.

Examiners: Prof. Dr. T.J. Schmidt, PSI Villigen/ETH Zürich
Prof. Dr. T. Lippert, PSI Villigen/ETH Zürich
Dr. P. Boillat, PSI Villigen

BACHELOR AND MASTER STUDENTS

Gong Chen
ETH Zürich

All-solid-state Li-ion Batteries based on sulfide solid electrolyte
June 2018 – January 2019
(Battery Materials and Diagnostics).

Victor Landgraf
Imperial College London, UK

Inverse Opal Derived Cathodes for Lithium-Sulfur Cells
October 2018 – May 2019
(Battery Electrodes and Cells).

Erik Samuelsson
KTH Royal Institute of Technology, Stockholm, Sweden

Hydrogen crossover suppression in polymer electrolyte water electrolyser systems
January – June 2019
(Membranes and Electrochemical Cells).

Eric Ricardo Carreón Ruiz
MaMaSELF, University of Montpellier, France

Energy Selective Neutron Imaging of Li-ion Battery Materials
February – July 2019
(Neutron Radiography of Electrochemical Systems).

Meriem Fikry
MaMaSELF, University of Rennes, France

Operando Decontamination Methods for Proton Exchange Membrane Electrolyzer
March – August 2019
(Neutron Radiography of Electrochemical Systems).

Franziska Jud
ETH Zürich

Liquid processing of sulfide based all-solid-state batteries
March – April 2019
(Battery Materials and Diagnostics).

André Müller
TU Braunschweig, Germany

Investigation of the Influence of Different Binders on the SEI of a Lithium-ion Battery by Means of OEMS
April - October 2019
(Battery Electrodes and Cells).

AWARDS

Marta Mirolo

2nd Best Poster Prize
M. Mirolo, X. Wu, C.A.F. Vaz, P. Novák, M. El Kazzi
Elucidation of the complex (de-)lithiation reactions of SnO_2 in all-solid-state batteries using operando X-ray photoelectron spectroscopy.

Condensed Matter Retreat, Windisch, Switzerland,
October 29-30, 2019.

Thomas Justus Schmidt

Christian Friedrich Schönbein Medal of Honor

EFCF2019 – European Fuel Cell Forum 2019, Lucerne,
Switzerland, July 5, 2019.

Fellow of Electrochemical Society 2019

The Electrochemical Society Meeting, Atlanta, GA, USA,
October 13–17, 2019.

CONFERENCES – SYMPOSIA

35th Swiss Electrochemistry Symposium, May 22, 2019.

On the Role of Batteries in Future Energy Systems

Organizers:
Felix N. Büchi, Cordelia Gloor, Electrochemistry Laboratory

Contributions from (in order of appearance):
Dirk Uwe Sauer, RWTH Aachen University, Aachen, Germany
Rosa Palacín, Institute of Material Science of Barcelona, Spain
Daniel Abraham, Argonne National Laboratory, Lemont, IL, USA
Detlef Stolten, Forschungszentrum Jülich, Germany
Olaf Conrad, JenaBatteries GmbH, Jena, Germany
Daniel Chartouni, ABB Corporate Research, Baden-Dättwil, Switzerland

From left to right: *Petr Novák, Olaf Conrad, Pierre Boillat, Lorenz Gubler, Dirk Uwe Sauer, Cordelia Gloor, Detlef Stolten, Rosa Palacín, Thomas J. Schmidt, Ursula Ludgate, Daniel Abraham, Sigita Trabesinger, Daniel Chartouni, Felix N. Büchi.*
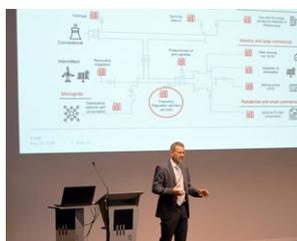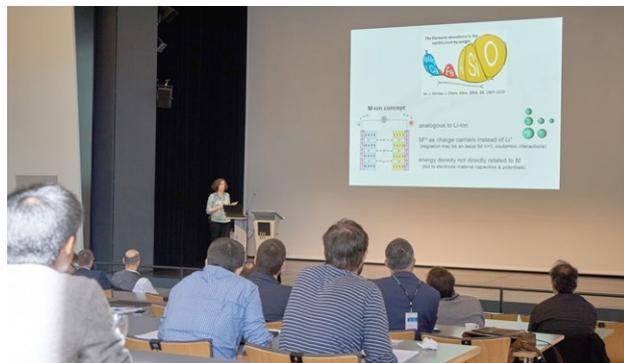
Plenary talks, poster session, lunch and discussions …

DOCUMENTATION

Collaborations with Industrial Partners

The Laboratory had the pleasure to collaborate with the following industrial partners during the year 2019:

Project Collaborations with External Partners

The Laboratory had the pleasure to collaborate with the following external partners during the year 2019:
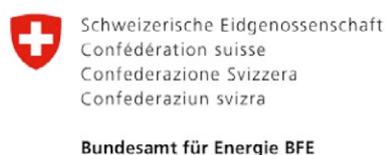
Teaching Activities

Teaching

Dr. E. Fabbri / PD Dr. L. Gubler / Dr. J. Herranz / Dr. S. Trabesinger	*Hands-on Electrochemistry for Energy Storage and Conversion Applications* PSI/ETH Zürich, FS 2019.
Prof. Dr. P. Novák	*Elektrochemie* ETH Zürich, HS 2019.
Prof. Dr. T.J. Schmidt / PD Dr. L. Gubler	*Renewable Energy Technologies 2* ETH Zürich, FS 2019.
Prof. Dr. T.J. Schmidt	*Physical Electrochemistry & Electrocatalysis* ETH Zürich, FS 2019.

Contributions to Courses

Dr. E. Fabbri / Dr. V. Saveleva	*Renewable Energy Technologies 2* ETH Zürich, FS 2019.
PD Dr. L. Gubler	*Energy Storage Systems* Lucerne University of Applied Sciences and Arts, May 15, 2019.

Publications

Peer Reviewed Papers

D.F. Abbott, R.K. Pittkowski,
K. Macounova, R. Nebel,
E. Marelli, E. Fabbri, I.E. Castelli,
P. Krtil, T.J. Schmidt
Design and Synthesis of Ir/Ru Pyrochlore Catalysts for the Oxygen Evolution Reaction Based on Their Bulk Thermodynamic Properties
ACS Applied Materials & Interfaces **11**, 37748–37760 (2019).

U. Babic, E. Nilsson, A. Pătru,
T.J. Schmidt, L. Gubler
Proton Transport in Catalyst Layers of a Polymer Electrolyte Water Electrolyzer: Effect of Anode Catalyst Loading
J. Electrochem. Soc. **166**, F214–F220 (2019).

U. Babic, M. Zlobinski,
T.J. Schmidt, P. Boillat, L. Gubler
CO$_2$-Assisted Regeneration of a Polymer Electrolyte Water Electrolyzer Contaminated with Metal Ion Impurities
J. Electrochem. Soc. **166**, F610–F619 (2019).

J. Billaud, D. Sheptyakov,
S. Sallard, D. Leanza, M. Talianker,
J. Grinblat, H. Sclar, D. Aurbach,
P. Novák, C. Villevieille
Li/Fe substitution in Li-rich Ni, Co, Mn oxides for enhanced electrochemical performance as cathode materials
Journal of Materials Chemistry A **7**, 15215–15224 (2019).

M. Bührer, M. Stampanoni,
X. Rochet, F. Büchi, J. Eller,
F. Marone
High-numerical-aperture macroscope optics for time-resolved experiments
Journal of Synchrotron Radiation **26**, 1161–1172 (2019).

C. Carminati, P. Boillat, F. Schmid,
P. Vontobel, J. Hovind,
M. Morgano, M. Raventos,
M. Siegwart, D. Mannes,
C. Gruenzweig, P. Trtik,
E. Lehmann, M. Strobl,
A. Kaestner
Implementation and Assessment of the Black Body Bias Correction in Quantitative Neutron Imaging
PLoS One **14**, e0210300 (24 pp.) (2019).

X. Cheng, B.J. Kim, E. Fabbri,
T.J. Schmidt
Co/Fe Oxyhydroxides Supported on Perovskite Oxides as Oxygen Evolution Reaction Catalyst Systems
ACS Applied Materials & Interfaces **11**, 34787–34795 (2019).

J.I.S. Cho, T.P. Neville, P. Trogadas,
Q. Meyer, Y. Wu, R. Ziesche,
P. Boillat, M. Cochet,
V. Manzi-Orezzoli, P. Shearing,
D.J.L. Brett, M.O. Coppens
Visualization of Liquid Water in a Lung-Inspired Flow-Field Based Polymer Electrolyte Membrane Fuel Cell via Neutron Radiography
Energy **170**, 14–21 (2019).

J. Conder, C. Vaulot, C. Marino,
C. Villevieille, C.M. Ghimbeu
Chitin and Chitosan—Structurally Related Precursors of Dissimilar Hard Carbons for Na-Ion Battery
ACS Applied Energy Materials **2**, 4841–4852 (2019).

J. Conder, C. Villevieille
How reliable is the Na metal as a counter electrode in Na-ion half cells?
Chemical Communications **55**, 1275–1278 (2019).

K. Ebner, J. Herranz, V.A. Saveleva,
B. Kim, S. Henning, M. Demicheli,
F. Krumeich, M. Nachtegaal,
T.J. Schmidt
Fe-Based O$_2$-Reduction Catalysts Synthesized Using Na$_2$CO$_3$ as a Pore-Inducing Agent
ACS Applied Energy Materials **2**, 1469–1479 (2019).

S. Erbach, B. Pribyl, M. Klages, L. Spitthoff, K. Borah, S. Epple, L. Gubler, A. Pătru, M. Heinen, T.J. Schmidt
Influence of operating conditions on permeation of CO_2 through the membrane in an automotive PEMFC system
International Journal of Hydrogen Energy **44**, 12760–12771 (2019).

S. Garbe, U. Babic, E. Nilsson, T.J. Schmidt, L. Gubler
Communication—Pt-Doped Thin Membranes for Gas Crossover Suppression in Polymer Electrolyte Water Electrolysis
Journal of The Electrochemical Society **166**, F873–F875 (2019).

E. Gilardi, A. Fluri, T. Lippert, D. Pergolesi
Real-time monitoring of stress evolution during thin film growth by in situ substrate curvature measurement
Journal of Applied Physics **125**, 082513 (2019).

L. Gubler
Membranes and Separators for Redox Flow Batteries
Curr. Opin. Electrochem. **18**, 31–36 (2019).

J. Halter, T. Gloor, B. Amoroso, T.J. Schmidt, F.N. Büchi
Wetting properties of porous high temperature polymer electrolyte fuel cells materials with phosphoric acid
Physical Chemistry Chemical Physics **21**, 13126–13134 (2019).

F. Haydous, M. Döbeli, W. Si, F. Waag, F. Li, E. Pomjakushina, A. Wokaun, B. Gökce, D. Pergolesi, T.K. Lippert
Oxynitride Thin Films versus Particle-Based Photoanodes: a Comparative Study for Photoelectrochemical Solar Water Splitting
ACS Applied Energy Materials **2** (1), 754–763 (2019).

F. Haydous, W. Si, V.A. Guzenko, F. Waag, E. Pomjakushina, M. El Kazzi, L. Sévery, A. Wokaun, D. Pergolesi, T. Lippert
Improved Photoelectrochemical Water Splitting of $CaNbO_2N$ Photoanodes by CoPi Photodeposition and Surface Passivation
The Journal of Physical Chemistry C **123**, 1059–1068 (2019).

M. He, K. Fic, E. Frąckowiak, P. Novák, E.J. Berg
Towards more Durable Electrochemical Capacitors by Elucidating the Ageing Mechanisms under Different Testing Procedures
ChemElectroChem **6**, 566–573 (2019).

F. Jeschull, F. Scott, S. Trabesinger
Interactions of silicon nanoparticles with carboxymethyl cellulose and carboxylic acids in negative electrodes of lithium-ion batteries
Journal of Power Sources **431**, 63–74 (2019).

F. Jeschull, Y. Surace, S. Zürcher, M.E. Spahr, P. Novák, S. Trabesinger
Electrochemistry and morphology of graphite negative electrodes containing silicon as capacity-enhancing electrode additive
Electrochimica Acta **320**, 134602 (2019).

B.J. Kim, E. Fabbri, D.F. Abbott, X. Cheng, A.H. Clark, M. Nachtegaal, M. Borlaf, I.E. Castelli, T. Graule, T.J. Schmidt
Functional Role of Fe-Doping in Co-Based Perovskite Oxide Catalysts for Oxygen Evolution Reaction
Journal of the American Chemical Society **141**, 5231–5240 (2019).

B.J. Kim, E. Fabbri, I.E. Castelli, M. Borlaf, T. Graule, M. Nachtegaal, T.J. Schmidt
Fe-Doping in Double Perovskite $PrBaCo_{2(1-x)}Fe_{2x}O_{6-\delta}$: Insights into Structural and Electronic Effects to Enhance Oxygen Evolution Catalyst Stability
Catalysts **9**, 263 (2019).

D. Leanza, M. Mirolo, C.A.F. Vaz, P. Novák, M. El Kazzi
Surface Degradation and Chemical Electrolyte Oxidation Induced by the Oxygen Released from Layered Oxide Cathodes in Li–Ion Batteries
Batteries & Supercaps **2**, 482–492 (2019).

D. Leanza, C.A.F. Vaz, G. Melinte, X. Mu, P. Novák, M. El Kazzi
Revealing the Dual Surface Reactions on a HE-NCM Li-Ion Battery Cathode and Their Impact on the Surface Chemistry of the Counter Electrode
ACS Applied Materials & Interfaces **11**, 6054–6065 (2019).

V. Manzi-Orezzoli, A. Mularczyk,
P. Trtik, J. Halter, J. Eller,
T.J. Schmidt, P. Boillat

Coating Distribution Analysis on Gas Diffusion Layers for Polymer Electrolyte Fuel Cells by Neutron and X-ray High-Resolution Tomography
ACS Omega **4**, 17236–17243 (2019).

F. Maxim, C. Contescu, P. Boillat,
B. Niceno, K. Karalis, A. Testino,
C. Ludwig

Visualization of Supercritical Water Pseudo-Boiling at Widom Line Crossover
Nature Communications **10**, 4114 (11 pp.) (2019).

Y. Nagai, J. Eller, T. Hatanaka,
S. Yamaguchi, S. Kato, A. Kato,
F. Marone, H. Xu, F.N. Büchi

Improving water management in fuel cells through microporous layer modifications: Fast operando tomographic imaging of liquid water
Journal of Power Sources **435**, 226809 (2019).

F.J. Oldenburg, E. Nilsson,
T.J. Schmidt, L. Gubler

Tackling Capacity Fading in Vanadium Redox Flow Batteries with Amphoteric Polybenz-imidazole/Nafion Bilayer Membranes
ChemSusChem **12**, 2920–2627 (2019).

F.J. Oldenburg, A. Ouarga,
T.J. Schmidt, L. Gubler

An Accelerated Stress Test Method for the Assessment of Membrane Lifetime in Vanadium Redox Flow Batteries
ACS Appl. Mater. Interfaces **11** (51), 47917–47928 (2019).

A. Pătru, T. Binninger, B. Pribyl,
T.J. Schmidt

Design Principles of Bipolar Electrochemical Co-Electrolysis Cells for Efficient Reduction of Carbon Dioxide from Gas Phase at Low Temperature
Journal of The Electrochemical Society **166**, F34–F43 (2019).

A.A. Permyakova, J. Herranz,
M. El Kazzi, J.S. Diercks, M. Povia,
L.R. Mangani, M. Horisberger,
A. Pătru, T.J. Schmidt

On the Oxidation State of Cu_2O upon Electrochemical CO_2 Reduction: An XPS Study
ChemPhysChem **20**, 3120–3127 (2019).

M. Povia, D.F. Abbott, J. Herranz,
A. Heinritz, D. Lebedev, B.-J. Kim,
E. Fabbri, A. Patru, J. Kohlbrecher,
R. Schäublin, M. Nachtegaal,
C. Copéret, T.J. Schmidt

Operando X-ray characterization of high surface area iridium oxides to decouple their activity losses for the oxygen evolution reaction
Energy & Environmental Science **12**, 3038–3052 (2019).

M.A. Safi, J. Mantzaras,
N.I. Prasianakis, A. Lamibrac,
F.N. Büchi

A pore-level direct numerical investigation of water evaporation characteristics under air and hydrogen in the gas diffusion layers of polymer electrolyte fuel cells
International Journal of Heat and Mass Transfer **129**, 1250–1262 (2019).

U. Sanyal, Y. Song, N. Singh,
J.L. Fulton, J. Herranz, A. Jentys,
O.Y. Gutiérrez, J.A. Lercher

Structure Sensitivity in Hydrogenation Reactions on Pt/C in Aqueous-phase
ChemCatChem **11**, 575–582 (2019).

S.F. Schneider, C. Bauer, P. Novák,
E.J. Berg

A modeling framework to assess specific energy, costs and environmental impacts of Li-ion and Na-ion batteries
Sustainable Energy & Fuels **3**, 3061–3070 (2019).

T. Schuler, R. De Bruycker,
T. Schmidt, F. Büchi

Polymer Electrolyte Water Electrolysis: Correlating Porous Transport Layer Structural Properties and Performance: Part I. Tomographic Analysis of Morphology and Topology
Journal of The Electrochemical Society **166**, F270–F281 (2019).

T. Schuler, T. Schmidt, F. Büchi

Polymer Electrolyte Water Electrolysis: Correlating Performance and Porous Transport Layer Structure: Part II. Electrochemical Performance Analysis
Journal of The Electrochemical Society **166**, F555–F565 (2019).

M. Siegwart, R.P. Harti, O. Manzi,
J. Valsecchi, M. Strobl,
C. Grünzweig, P. Boillat

Selective Visualization of Water in Fuel Cell Gas Diffusion Layers with Neutron Dark-Field Imaging
Journal of The Electrochemical Society **166**, F149 (2019).

M. Siegwart, R. Woracek,
J.I. Márquez Damián, A.S. Tremsin,
V. Manzi-Orezzoli, M. Strobl,
T.J. Schmidt, P. Boillat

Distinction Between Super-Cooled Water and Ice with High Duty Cycle Time-of-Flight Neutron Imaging
Review of Scientific Instruments **90**, 103705 (15 pp.) (2019).

Y. Surace, F. Jeschull, T. Schott,
S. Zürcher, M.E. Spahr,
S. Trabesinger

Improving the Cycling Stability of SnO$_2$–Graphite Electrodes
ACS Applied Energy Materials **2**, 7364–7374 (2019).

E.H.R. Tsai, J. Billaud, D.F. Sanchez,
J. Ihli, M. Odstrčil, M. Holler,
D. Grolimund, C. Villevieille,
M. Guizar-Sicairos

Correlated X-Ray 3D Ptychography and Diffraction Microscopy Visualize Links between Morphology and Crystal Structure of Lithium-Rich Cathode Materials
iScience **11**, 356–365 (2019).

J. Valsecchi, R.P. Harti,
M. Raventós, M.D. Siegwart,
M. Morgano, P. Boillat, M. Strobl,
P. Hautle, L. Holitzner, U. Filges,
W. Treimer, F.M. Piegsa,
C. Grünzweig

Visualization and Quantification of Inhomogeneous and Anisotropic Magnetic Fields by Polarized Neutron Grating Interferometry
Nat Commun **10**, 3788 (9 pp.) (2019).

X. Wu, J. Billaud, I. Jerjen,
F. Marone, Y. Ishihara, M. Adachi,
Y. Adachi, C. Villevieille, Y. Kato

Operando Visualization of Morphological Dynamics in All-Solid-State Batteries
Advanced Energy Materials **9**, 1901547 (2019).

Y. Wu, Q. Meyer, F. Liu, L. Rasha,
J.I.S. Cho, T.P. Neville,
J. Millichamp, R. Ziesche,
N. Kardjilov, P. Boillat,
H. Markötter, I. Manke, M. Cochet,
P. Shearing, D.J.L. Brett

Investigation of Water Generation and Accumulation in Polymer Electrolyte Fuel Cells Using Hydro-Electrochemical Impedance Imaging
Journal of Power Sources **414**, 272–277 (2019).

H. Xu, F. Marone, S. Nagashima,
H. Nguyen, K. Kishita, F.N. Büchi,
J. Eller

(Invited) Exploring Sub-Second and Sub-Micron X-Ray Tomographic Imaging of Liquid Water in PEFC Gas Diffusion Layers
ECS Transactions **92**, 11–21 (2019).

Talks

Invited Talks

P. Boillat

20 years of neutron imaging for fuel cells: what did we learn and what is yet to come?
FDFC-2019 – 8th International Conference on Fundamentals and Development of Fuel Cells, Nantes, France, February 12–14, 2019.

C. Bolli

Investigation of electrolyte additive reaction mechanisms by OEMS
Presentation at University of Freiburg, Freiburg, Germany, April 19, 2019.

C. Bolli

Highlights from OEMS investigations on lithium and sodium ion batteries
Presentation at Technical University of Braunschweig, Braunschweig, Germany, September 10, 2019.

F.N. Büchi

X-Ray Tomographic Imaging of PEFC's – Insight into water management
Institutskolloquium Technische Thermodynamik, DLR, Struttgart, Germany, May 16, 2019.

F.N. Büchi

Insights from the inside: Imaging Water in the Porous Structures of Fuel Cells
235th ECS Meeting, Dallas, USA, May 28, 2019.

F.N. Büchi

Understanding and optimizing water transport in gas diffusion layers
Symposium on Insights into Gas Diffusion Electrodes, Magdeburg, Germany, September 23, 2019.

F.N. Büchi

Application of fuel cells for UPS
Workshop Energy for Sustainable Science, Villigen PSI, Switzerland, November 28, 2019.

M. El Kazzi

Photoemission Spectroscopy in Battery Research
International Summer School on Materials for Energy Storage and Conversion, Mugla Sıtkı Kocman University, Turkey, September 7–11, 2019.

M. El Kazzi

Operando XPS for a Direct Monitoring of the Chemical and Electronic Properties of the Electrolyte-Electrode Interfaces in All-Solid-State Batteries
mESC-IS, Akyaka-Mugla, Turkey, September 11–13, 2019.

M. El Kazzi

Nanoscale XPEEM Spectroscopy Unveils the Complex Local (Electro-) Chemical Surface Reactions of Cycled Electrodes in Li-Ion Batteries
ECS-2019 – 236th The Electrochemical Society Meeting, Atlanta, USA, October 13–17, 2019.

L. Gubler

Amphoteric and Bilayer Membranes for Vanadium Redox Flow Batteries
Asilomar Conference on Polymers for Fuel Cells, Energy Storage, and Conversion, Pacific Grove, CA, USA, February 24–27, 2019.

L. Gubler, A. Pătru,
B. Pribyl-Kranewitter,
A. Muroyama

CO2 as Feedstock for Value-Added Products: the Potential Role of Electrochemistry
Seminar at the Shell Technology Centre, Amsterdam, The Netherlands, October 3, 2019.

P. Novák

Operando Characterization of Battery Materials
Seminar at Apple Inc., Cupertino, CA, USA, February 26, 2019.

P. Novák

Raman Microscopy: What Can the Technique Tell Us?
IBA-2019 – International Battery Association Meeting, La Jolla, CA, USA, March 5, 2019.

P. Novák	*Energy Storage in Batteries: Facts versus Wishful Thinking* Advanced Battery Power Conference, Aachen, Germany, April 3, 2019.
P. Novák	*Modern Analytical Tools to Study Interfaces and Interphases in Lithium-Ion Batteries* Power our Future 2019 - The 4th International Forum on Progress and Trends in Battery and Capacitor Technologies, Vitoria-Gasteiz, Spain, July 3, 2019.
P. Novák	*Battery Materials and Their Operando Characterization* Seminar in Materials Colloquium of ETH, Zurich, Switzerland, October 2, 2019.
P. Novák	*Comparing Performance, Costs, and Environmental Impact of Li-Ion and Na-Ion batteries* ABAA 12 – Advanced Lithium Batteries for Automobile Applications, Ulm, Germany, October 9, 2019.
F.J. Oldenburg	*Ion Exchange Membranes for Redox Flow Batteries* RFB Kolloqium 2019, Karlsruhe, Germany, September 25, 2019.
S. Trabesinger	*Silicon as electrode and as electrode's capacity-enhancing additive* INESS-2019 – International Conference on Nanomaterials and Advanced Energy Storage Systems, Almaty, Kazakhstan, August 7–9, 2019.
C. Villevieille	*Operando Investigation of All-Solid-State-Batteries Using Li_3PS_4 Solid Electrolyte* IBA – International Battery Conference, La Jolla CA, USA, March 3–8 2019.
C. Villevieille	*Mechanical vs. chemical stability of All-Solid-State-Batteries. Which one is the biggest challenge to tackle?* E-MRS – European Materials Research Spring Meeting, Nice, France, May 24 – June 1, 2019.
T.J. Schmidt	*Polymer Electrolyte Fuel Cells Catalysis – Older Goodies and New Concepts* 235th ECS Spring Meeting, Dallas, TX, USA, May 28, 2019.
T.J. Schmidt	*Energy Research at Paul Scherrer Institute: Hydrogen Technologies and more* National Renewable Energy Laboratory, Golden, CO, USA, June 3, 2019.
T.J. Schmidt	*From Hydrogen to Fuel Cells. The Journey of a Catalyst* EFCF 2019, Low-Temperature Fuel Cells, Electrolysers & H_2 Processing. Fundamentals and Engineering Design, Lucerne, Switzerland, July 5, 2019.
T.J. Schmidt	*Power to X: Perspectives for Switzerland* World Energy Council, Zurich, Switzerland, August 18, 2019.
T.J. Schmidt	*Operando Studies of Oxygen Evolution Catalysts* Workshop Interdisciplinarity in Electrochemistry, Technical University Munich, Germany, September 24, 2019.
T.J. Schmidt	*Research on Sustainable Energy at PSI* 5th Workshop Energy for Sustainable Science at Large Research Infrastructures, Paul Scherrer Institut, Villigen, Switzerland, November 28, 2019.

Contributed Talks

U. Babic, M. Zlobinski, P. Boillat, T.J. Schmidt, L. Gubler	*Contamination Effects in Polymer Electrolyte Water Electrolyzers* ICE – 2nd International Conference on Electrolysis, Loen, Norway, June 9–13, 2019.
P. Boillat, M. Siegwart, R. Carreon, M. Zlobinski, M. Cochet	*Broad Pulse Time-of-Flight Neutron Imaging: Current and Future Applications in Electrochemistry* NEUWAVE-10 – 10th Workshop on NEUtron WAVElength Dependent Imaging, Villigen, Switzerland, May 26–29, 2019.
P. Boillat, F.N. Büchi, L. Gubler, T.J. Schmidt	*Use and Misuse of Electrochemical Impedance Spectroscopy (EIS) in Fuel Cell Research* ECS-2019 – 236th The Electrochemical Society Meeting, Atlanta, USA, October 13–17, 2019.
F. N. Büchi, C. Csoklich	*Structuring GDL's for Improved Water Management* ECS-2019 – 236th The Electrochemical Society Meeting, Atlanta, USA, October 16, 2019.
M. Cochet, V. Manzi-Orezzoli, D. Scheuble, P. Boillat	*Experimental Proof of Concept for an Innovative Evaporative Cooling Concept for Polymer Electrolyte Fuel Cells* ECS-2019 – 236th The Electrochemical Society Meeting, Atlanta, USA, October 13–17, 2019.
J.S. Diercks, J. Herranz, D. Perego, T.J. Schmidt	*Pd-based nanoparticles and bimetallic aerogels for the efficient electroreduction of CO_2 to added-value products* SCCER Meeting, Villars-sur-Ollon, Switzerland, January 29–30, 2019.
J.S. Diercks, M. Georgi, J. Herranz, A. Eychmüller, T.J. Schmidt	*Pd-based nanoparticles and bimetallic aerogels for the efficient electroreduction of CO_2 to added value products* PECAS, Donostia-San Sebastián, Spain, August 27–30, 2019.
K. Ebner, V.A. Saveleva, L. Ni, U.I. Kramm, A. Zitolo, J. Li, F. Jaouen, E. Marelli, M. Medarde, D. Klose, G. Smolentsev, O.V. Safonova, M. Nachtegaal, T.J. Schmidt, J. Herranz	*X-ray Emission Spectroscopy Insights into the Spin State of Iron in Fe/N/C Catalysts* EFCD-2019 – Electrolysis and Fuel Cell Discussions, La Grande Motte, France, September 15–18, 2019.
F.N. Büchi, M. Bührer, F. Marone, T.J. Schmidt, J. Eller	*X-Ray Tomographic imaging of liquid water in gas diffusion layers at 10 Hz* ModVal-2019 – 16th Symposium on Modeling and Experimental Validation of Electrochemical Energy Technologies, Braunschweig, Germany, March 12–13, 2019.
F.N. Büchi, T.J. Schmidt	*Characterization of PTL topology and PTL/CL interface* IEA Annex 30 Electrolysis Workshop, Hannover, Germany, March 29, 2019.
F.N. Büchi, T.J. Schmidt	*Structuring GDL's for Improved Water Management* ECS-2019 – 236th The Electrochemical Society Meeting, Atlanta, USA, October 13–17, 2019.
F.N. Büchi, T.J. Schmidt	*On the role of the porous transport layer structure in polymer electrolyte water electrolysis* ECS-2019 – 236th The Electrochemical Society Meeting, Atlanta, USA, October 13–17, 2019.
F.N. Büchi, T. Schuler	*On the Role of the Porous Transport Layer Structure in Polymer Electrolyte Water Electrolysis* ECS-2019 – 236th The Electrochemical Society Meeting, Atlanta, USA, October 13–17, 2019.

L. Gubler, F.J. Oldenburg,
A. Ouarga, T.J. Schmidt

An Accelerated Stress Test for Flow Battery Membranes
EMEA 2019 – Workshop on Ion Exchange Membranes for Energy Applications, Bad Zwischenahn, Germany, June 25–27, 2019.

J. Herranz, M. Povia, D.F. Abbott,
D. Lebedev, M. Nachtegaal,
C. Copéret, T.J. Schmidt

Operando X-ray Characterization of High Surface Area Ir-Oxides to Decouple their OER-Activity Losses
EFCD-2019 – Electrolysis and Fuel Cell Discussions, La Grande Motte, France, September 15–18, 2019.

L. Höltschi, C. Jordy, V. Pelé, F. Jud,
C. Villevieille, M. El Kazzi, P. Novák

Combining Operando Techniques to Identify Challenges in Graphite Composite Negative Electrodes for Sulfide Based Solid-State Lithium Batteries
ECEE-2019 – Electrochemical Conference on Energy and the Environment, Glasgow, United Kingdom July 21–26, 2019.

L. Höltschi, C. Jordy, V. Pelé, F. Jud,
C. Villevieille, M. El Kazzi, P. Novák

Elucidating the Performance Limitations of Graphite as Negative Electrode for Sulfide Based Solid State Batteries
2nd Swiss and Surrounding Battery Days, Dübendorf, Switzerland, August 26–28, 2019.

L. Höltschi, C. Jordy, V. Pelé, F. Jud,
C. Villevieille, M. El Kazzi, P. Novák

Combining Operando Techniques to Identify Challenges in Graphite Composite Negative Electrodes for Sulfide Based Solid-State Lithium Batteries
Laboratory of Inorganic Chemistry Christmas Symposium, Zürich, Switzerland, December 11, 2019.

V. Manzi-Orezzoli, M. Siegwart,
T.J. Schmidt, P. Boillat

Bypassing the Jam: How GDLs with Engineered Water Highways Can Re-Enable Interdigitated Flow Fields for PEFCs
ECS-2019 – 236th The Electrochemical Society Meeting, Atlanta, USA, October 13–17, 2019.

M. Mirolo, X. Wu, C.A.F. Vaz,
P. Novák, M. El Kazzi

Elucidating the complex (de-)lithiation reactions of SnO_2 in all SSB using operando XPS
2nd Swiss and Surrounding Battery Days, Dübendorf, Switzerland, August 27, 2019.

M. Mirolo, X. Wu, C. A. F. Vaz,
P. Novák, M. El Kazzi

Operando XPS for a Direct Monitoring of the Solid Electrolyte Stability and (De-)Lithiation Reactions of SnO_2 in All Solid-State Batteries
LiBD-2019 – Lithium Batteries Discussion Conference on Electrode Materials, Arcachon, France, September 15–20, 2019.

M. Mirolo, C.A.F. Vaz, P. Novák,
M. El Kazzi

Disclosing the complex surface reactivity of $LiNi_{0.8}Co_{0.15}Al_{0.05}O_2$ at high potential by combining XPEEM, XAS and XPS measurements
ECS-2019 – 236th The Electrochemical Society Meeting, Atlanta, USA, October 13–17, 2019.

M. Mirolo, X. Wu, C.A.F. Vaz,
P. Novák, M. El Kazzi

Elucidation of the complex (de-)lithiation reactions of SnO_2 in all solid-state battery using operando X-ray photoelectron spectroscopy
ECS-2019 – 236th The Electrochemical Society Meeting, Atlanta, USA, October 13–17, 2019.

A. Mularczyk, F.N. Büchi,
T.J. Schmidt, J. Eller

Convective Flow in Fuel Cell Gas Diffusion Layers and its Impact on Evaporation
11th Annual Meeting InterPore, Valencia, Spain, May 6–10, 2019.

F.J. Oldenburg

An Accelerated Stress Test for Flow Battery Membranes
IFBF 2019 – International Flow Battery Forum, Lyon, France, June 25–27, 2019.

S. Schneider, C. Bauer, P. Novák,
E.J. Berg

A modeling framework to assess specific energy, costs and environmental impacts of Li-ion and Na-ion batteries
ModVal-2019 – 16th Symposium on Modeling and Experimental Validation of Electrochemical Energy Technologies, Braunschweig, Germany, March 12–13, 2019.

S. Schneider, P. Novak, T. Kober	*Rechargeable batteries for simultaneous demand peak shaving and price arbitrage* International Energy Workshop 2019, Paris, France, June 3–5, 2019.
T. Schuler, T.J. Schmidt, F.N. Büchi	*Correlation of Structural Porous Transport Layer Properties for Polymer Electrolyte Water Electrolysis* ICIEIEP-2019 – International Conference on Industrial Electrolysis, Barcelona, Spain, May 22–25, 2019.
T. Schuler, R. De Bruycker, T.J. Schmidt, F.N. Büchi	*The Role of Interface Properties and Polymer Electrolyte Water Electrolysis Performance* ICE – 2nd International Conference on Electrolysis, Loen, Norway, June 9–13, 2019.
T. Schuler, T.J. Schmidt, F.N. Büchi	*Correlation of Porous Transport Layers Properties and Polymer Electrolyte Water Electrolysis Performance* EFCF-2019 – European Fuel Cell Forum, Lucerne, Switzerland July 2–5, 2019.
M. Siegwart, J. Valsecchi, C. Grünzweig, M. Strobl, T.J. Schmidt, P. Boillat	*Optimized Neutron Grating Interferometer for the Visualization of Water in Fuel Cell Materials* NEUWAVE-10 – 10th Workshop on NEUtron WAVElength Dependent Imaging, Villigen, Switzerland, May 26–29, 2019.
M. Striednig, M. Cochet, P. Boillat, T.J. Schmidt, F.N. Büchi	*Evaporative Cooling of Polymer Electrolyte Fuel Cells – Potentials and Limits* ModVal-2019 – 16th Symposium on Modeling and Experimental Validation of Electrochemical Energy Technologies, Braunschweig, Germany, March 12–13, 2019.
M. Striednig, M. Cochet, P. Boillat, T.J. Schmidt, F.N. Büchi	*Potentials and Limits of Evaporative Cooling for Polymer Electrolyte Fuel Cells* SCCER Mobility Young Talent Development Seminar Series, Zürich, Switzerland, April 23. 2019.
M. Striednig, M. Cochet, P. Boillat, T.J. Schmidt, F.N. Büchi	*Potentials and Limits of Evaporative Cooling for Polymer Electrolyte Fuel Cells* EFCF-2019 – European Fuel Cell Forum, Lucerne, Switzerland, July 2–5, 2019.
M. Striednig, M. Cochet, P. Boillat, T.J. Schmidt, F.N. Büchi	*A Model Based Analysis of Evaporative Cooling for Polymer Electrolyte Fuel Cells* ECS-2019 – 236th The Electrochemical Society Meeting, Atlanta, USA, October 13–17, 2019.
X. Wu, M. Mirolo, C. Villevieille, P. Novák, M. El Kazzi	*Operando XPS for a Direct Monitoring of the Chemical and Electronic Properties of the Electrolyte-Electrode Interfaces in All-Solid-State Batteries* 35th SOAG – The Surface Science and Thin Films Community of Switzerland, Fribourg University, Fribourg, Switzerland, January 31, 2019.
H. Xu, M. Bührer, F. Marone, T.J. Schmidt, F.N. Büchi, J. Eller	*10 Hz Operando X-ray Tomographic Imaging of Liquid Water in Gas Diffusion Layers of Polymer Electrolyte Fuel Cells* Interpore Conference 2019, Valencia, Spain, May 6–10, 2019.
H. Xu, M. Bührer, F. Marone, S. Nagashima, K. Kishita, F.N. Büchi, J. Eller	*Sub-second X-ray Tomographic Imaging of Liquid Water Dynamics in PEFC Gas Diffusion Layers* ECS-2019 – 236th The Electrochemical Society Meeting, Atlanta, USA, October 13–17, 2019.
L. Zhang, C. Bolli, H. Sommer, P. Novák, S. Trabesinger	*Elucidating the degradation of Ni-rich layered oxides in humid environment* 2nd Swiss and Surrounding Battery Days, Dübendorf, Switzerland, August 26–28, 2019.
L. Zhang, C. Bolli, H. Sommer, M. El Kazzi, P. Novák, S. Trabesinger	*Elucidating the degradation of Ni-rich layered oxide in humid environment* LiBD-2019 – Lithium Batteries Discussion Conference on Electrode Materials, Arcachon, France, September 5, 2019.
L. Zhang, C. Bolli, H. Sommer, M. El Kazzi, P. Novák, S. Trabesinger	*Elucidating the degradation of Ni-rich layered oxide in humid environment* MRS-2019 – Materials Research Society Fall Meeting, Boston, USA, December 6, 2019.

M. Zlobinski, F. Büchi,
T.J. Schmidt, P. Boillat

High resolution and sub-second Neutron imaging of porous transport layers of proton exchange membrane water electrolyser
ICE – 2nd International Conference on Electrolysis, Loen, Norway, June 9–13, 2019.

M. Zlobinski, L. Gubler,
T.J. Schmidt, P. Boillat

Operando Sub-Second Neutron Imaging of Cationic Species Migration in a Proton Exchange Membrane Water Electrolyzer
ECS-2019 – 236th The Electrochemical Society Meeting, Atlanta, USA, October 13–17, 2019.

Patents

T. Schuler, F.N. Büchi

Porous Transport Layer Based on Multiple Micro and Nano Sintered Porous Layers
2019P00557EP, filed January 23, 2019.

A. Schuller, J. Eller

Non-invasive method and system for ionomer conductivity determination in polymer electrolyte fuel cells
2019P04382EP, filed February 2, 2019.

S. Garbe, U. Babic, L. Gubler,
T.J. Schmidt

Method for Preparing a Polymer Membrane for a Polymer Electrolyte Water Electrolyser
EP19175071.0, filed May 17, 2019.

Posters

D. Aegerter, B.-J. Kim, E. Fabbri,
M. Borlaf, T. Graule, T.J. Schmidt

The Effect of Fe in $Ba_{0.5}Sr_{0.5}Co_xFe_{1-x}O_{3-\delta}$ Towards the Oxygen Evolution Reaction in Alkaline Media
EFCF-2019 – European Fuel Cell Forum, Lucerne, Switzerland, July 2–5, 2019.

C. Bolli, M. He, A. Guéguen,
M. Mendez, E.J. Berg, P. Novák

Online Electrochemical Mass Spectrometry for Rechargeable Batteries
IBA-2019 – International Battery Association Meeting, La Jolla, USA, March 3–8, 2019.

C. Bolli, L. Zhang, M. Goktas,
M. He, A. Guéguen, M. Mendez,
P. Novák, P. Adelhelm, E.J. Berg,
S. Trabesinger

Online Electrochemical Mass Spectrometry for Li- and Na-ion Batteries
2nd Swiss and Surrounding Battery Days, Dübendorf, Switzerland, August 26–28, 2019.

P. Chauhan, K. Hiekel, D. Perego,
J. Herranz, A. Eychmüller,
T.J. Schmidt

Quantifying the Electrochemical Surface Area of Au Aerogels as Prospective CO_2 Electroreduction Catalysts
PECAS 2019 – Photo- and ElectroCatalysis at the Atomic Scale, Donostia-San Sebastián, Basque Country, Spain, August 27–30, 2019.

J.S. Diercks, J. Herranz, D. Perego,
T.J. Schmidt

Pd-based nanoparticles and bimetallic aerogels for the efficient electroreduction of CO_2 to added-value products
SCCER Meeting, Villars-sur-Ollon, Switzerland, January 29–30, 2019.

J.S. Diercks, M. Georgi, J. Herranz,
A. Eychmüller, T.J. Schmidt

Pd-based nanoparticles and bimetallic aerogels for the efficient electroreduction of CO_2 to added value products
PECAS 2019 – Photo- and ElectroCatalysis at the Atomic Scale, Donostia-San Sebastián, Basque Country, Spain, August 27–30, 2019.

K. Ebner, V.A. Saveleva, J. Herranz, B. Kim, T.J. Schmidt	*Using Na_2CO_3 as an inexpensive pore inducing agent for Fe/N/C-type ORR catalysts* Electrochemical Discussions: latest insights on PGM-free catalysts for Energy Systems and Fuel Cells, Turin, Italy, February 8, 2019.
K. Ebner, V.A. Saveleva, L. Ni, A.H. Clark, M. Nachtegaal, U.I. Kramm, T.J. Schmidt, J. Herranz	*[57]Fe-enrichment effect on the composition and performance of Fe-based O_2-reduction electrocatalysts* EFCD-2019 – Electrolysis & Fuel Cell Discussions, La Grande Motte, France, September 15–18, 2019.
K. Ebner, V.A. Saveleva, L. Ni, U.I. Kramm, A. Zitolo, J. Li, F. Jaouen, E. Marelli, M. Medarde, D. Klose, G. Smolentsev, O.V. Safonova, M. Nachtegaal, T.J. Schmidt, J. Herranz	*X-ray Emission Spectroscopy Insights into the Spin State of Iron in Fe/N/C Catalysts* EFCD-2019 – Electrolysis & Fuel Cell Discussions, La Grande Motte, France, September 15–18, 2019.
J. Eller	*Spatially resolved analysis of saturation dependent operando GDL gas phase transport properties in PEFCs* ModVal 2019 – 16th Symposium on Modeling and Experimental Validation of Electrochemical Energy Technologies, Braunschweig, Germany, March 12–13, 2019.
S. Garbe, U. Babic, T.J. Schmidt, L. Gubler	*Hydrogen Cross-over Suppression in PEWE through Pt-doped Thin Membranes* ICE – 2nd International Conference on Electrolysis, Loen, Norway, June 9–14, 2019.
S. Garbe, U. Babic, T.J. Schmidt, L. Gubler	*Hydrogen Cross-over Suppression in PEWE through Pt-doped Thin Membranes* Power2Gas Conference, Marseille, France, October 23–24, 2019.
J. Herranz, M. Povia, D.F. Abbott, D. Lebedev, M. Nachtegaal, C. Copéret, T.J. Schmidt	*Operando X-ray Characterization of High Surface Area Ir-Oxides to Decouple their OER-Activity Losses* EFCD-2019 – Electrolysis and Fuel Cell Discussions, La Grande Motte, France, September 15–18, 2019.
L. Höltschi, M. Cochet, P. Trtik, C. Jordy, C. Villevieille, P. Boillat	*Operando Neutron Imaging for Next-Generation Solid State Batteries* IBA-2019 – International Battery Association Meeting, San Diego, USA, March 3–8, 2019.
L. Höltschi, C. Jordy, V. Pelé, F. Jud, C. Villevieille, M. El Kazzi, P. Novák	*Exploring the Limits of Graphite as Negative Electrode for Sulfide based Solid-State Lithium Batteries* 35th Swiss Electrochemistry Symposium, Aarau, Switzerland, May 22, 2019.
L. Höltschi, C. Jordy, V. Pelé, F. Jud, C. Villevieille, M. El Kazzi, P. Novák	*Exploring the Limits of Graphite as Negative Electrode for Sulfide based Solid-State Lithium Batteries* 2nd Swiss and Surrounding Battery Days, Dübendorf, Switzerland, August 26–28, 2019.
F. Jeschull, F. Scott, S. Trabesinger	*Interactions of silicon nanoparticles with carboxymethyl cellulose and carboxylic acids in Li-ion battery negative electrodes* IBA-2019 – International Battery Association Meeting, La Jolla, USA, March 3–8, 2019.
D. McNulty, S. Trabesinger	*Sulfur-infilled carbon inverse-opals for lithium–sulfur batteries* 2nd Swiss and Surrounding Battery Days, Dübendorf, Switzerland, August 26–28, 2019.
D. McNulty, S. Trabesinger	*Carbon inverse opals as a sulfur host for advanced lithium–sulfur batteries* ECS-2019 – 236th The Electrochemical Society Meeting, Atlanta, USA, October 16, 2019.
M. Mirolo, C.A.F. Vaz, P. Novák, M. El Kazzi	*Electrodes surface evolution and cross-talk processes in a full cell NCA vs. LTO revealed by XPEEM* 35th Swiss Electrochemistry Symposium, Aarau, Switzerland, May 22, 2019.

M. Mirolo, C.A.F. Vaz, P. Novák, M. El Kazzi

Disclosing the complex surface reactivity of NCA at high potential by combining XPEEM, XAS and XPS measurements
2nd Swiss and Surrounding Battery Days, Dübendorf, Switzerland, August 26–28, 2019.

M. Mirolo, X. Wu, C.A.F. Vaz, P. Novák, M. El Kazzi

Elucidation of the complex (de-)lithiation reactions of SnO_2 in all-solid-state batteries using operando X-ray photoelectron spectroscopy
Condensed Matter Retreat, Windisch, Switzerland, October 29–30, 2019.

A. Mularczyk, F.N. Büchi, T.J. Schmidt, J. Eller

How mass transport drives evaporation in gas diffusion layers of polymer electrolyte fuel cell
ModVal 2019 – 16th Symposium on Modeling and Experimental Validation of Electrochemical Energy Technologies, Braunschweig, Germany, March 12–13, 2019.

F.J. Oldenburg, A. Ouarga, T.J. Schmidt, L. Gubler

An Accelerated Stress Test Method for the Assessment of Membrane Lifetime in Vanadium Flow Batteries
Asilomar Conference on Polymers for Fuel Cells, Energy Storage, and Conversion, Pacific Grove CA, USA, February 24–27, 2019.

H.Q. Pham, S. Trabesinger

A novel electrolyte additive for improving the interfacial stability of Ni-rich cathodes for high-energy lithium-ion batteries
2nd Swiss and Surrounding Battery Days, Dübendorf, Switzerland, August 26, 2019.

B. Pribyl, J.S. Diercks, J. Herranz, A. Patru, T.J. Schmidt

Efficient CO_2-Reduction: From catalyst development to industrial application
D-CHAB Evaluation, Zürich, Switzerland, May 7, 2019.

M. Striednig, M. Cochet, P. Boillat, T.J. Schmidt, F.N. Büchi

Potentials and Limits of Evaporative Cooling for Polymer Electrolyte Fuel Cells
SCCER Mobility Annual Conference 2019, Zürich, Switzerland, September 6, 2019.

D. Vonlanthen, A. Schneider, F.J. Oldenburg, T.J. Schmidt, L. Gubler

Low-Cost Nano-Polyelectrolyte-Separators (NPS) for Selective and Efficient Ion-Transport in Redox-Flow Batteries
Gordon Research Conference on Nanomaterials for Applications in Energy Technology – Challenges and Opportunities at the Nanoscale: Applications, Simulation, Advanced Characterization and Novel Manufacturing, Ventura CA, USA, February 24 – March 1, 2019.

D. Vonlanthen, A. Schneider, F.J. Oldenburg, T.J. Schmidt, L. Gubler

Low-Cost Nano-Polyelectrolyte-Separators for Selective and Efficient Ion-Transport in Redox-Flow Batteries
IFBF 2019 – International Flow Battery Forum, Lyon, France, July 9–11, 2019.

L. Zhang, C. Tsolakidou, S. Trabesinger

Operando gas analysis in Na-ion batteries
8th SCCER HaE Symposium, Dübendorf, Switzerland, November 5, 2019.

M. Zlobinski, P. Boillat, T.J.Schmidt

Neutron imaging of PTLs of PEM water electrolysers in high-resolution and low-exposure time modes
35th Swiss Electrochemistry Symposium, Aarau, Switzerland, May 22, 2019.

Conferences & Workshops Organizations

F.N. Büchi, C. Gloor	*35th Swiss Electrochemistry Symposium: On the Role of Batteries in Future Energy Systems* Kultur- und Kongresshaus KuK, Aarau, Switzerland, May 22, 2019.
F.N. Büchi, T.J. Schmidt	*19th Symposium on Polymer Electrolyte Fuel Cells & Eletrolysis PEFC & EC19* 236th ECS Fall Meeting, Atlanta, GA, USA, October 13–17, 2019. Members of Organizing Committee
T.J. Schmidt	*5th Workshop Energy for Sustainable Science at large Research Structures* Paul Scherrer Institut, Villigen, Switzerland, November 28–29, 2019. Member of Organizing Committee

Editorial Work

F.N. Büchi, T.J. Schmidt (Co-Editors)	*Polymer Electrolyte Fuel Cells & Electrolysis 19 (PEFC & EC 19)* ECS Transactions **92** (8), The Electrochemical Society, Pennington, NJ, USA (2019).
C. Gloor, P. Lutz, F.N. Büchi, L. Gubler, T.J. Schmidt, C. Villevieille	*PSI Electrochemistry Laboratory Annual Report 2018* doi: 10.3929/ethz-a-007047464, ISSN 1661–5379